

University of South Alabama

JagWorks@USA

Undergraduate Honors Theses

Honors College

8-2023

Exogenous Exposure to Dihydroxyacetone Mimics High Fructose Induced Oxidative Stress and Mitochondrial Dysfunction

Raj Mehta

Follow this and additional works at: https://jagworks.southalabama.edu/honors_college_theses



Part of the [Chemical Actions and Uses Commons](#), [Chemical and Pharmacologic Phenomena Commons](#), [Medical Biochemistry Commons](#), [Organic Chemicals Commons](#), [Other Medical Sciences Commons](#), and the [Other Medicine and Health Sciences Commons](#)

Exogenous exposure to dihydroxyacetone mimics high fructose induced oxidative stress and
mitochondrial dysfunction

By

Raj Mehta

A thesis submitted in partial fulfillment of the requirements of the Honors College at
University of South Alabama and the Bachelor of Sciences in the Biomedical
Sciences Department

University of South Alabama

Mobile

August 2023

Approved by:

Mentor: Glen Borchert

Committee Member: Kelly Major

Committee Member: Timothy Sherman

Douglas Marshall,
Dean of Honors College

2023
Raj Mehta
ALL RIGHTS RESERVED

Dedication

This thesis is dedicated to my parents Vipul Mehta and Lina Mehta for their support throughout my life. My parents have been my fuel to achieving academic success and I hope to continue to impress them. The unconditional love they have provided me has immensely helped me get through any obstacles I have encountered. I am eternally grateful for them as they have sustained my optimism through difficult times. I would not be here without the support of my parents. I also would like to thank Dr. Gassman and Dr. Borchert for being excellent mentors that have guided me through most of the academic success I have achieved as an undergraduate. I hope to foster these relationships throughout all parts of my future career. It is comforting to know that there are always mentors to guide students through all obstacles that they face in life.

Acknowledgements

I cannot thank Dr. Gassman and Dr. Borchert enough for the immense guidance they have provided me throughout my career as an undergraduate student at USA. It has been my honor to work alongside these experts in their fields, and they have greatly influenced my desire to become a physician. I would like to extend this appreciation to my thesis committee members Dr. Marshall, Dr. Sherman, and Dr. Major for giving me the opportunity to present my research. I want to thank the USA Biology and Biomedical Sciences Departments as well as the USA Honors College for their continued support throughout my journey as an undergraduate.

Abstract

Dihydroxyacetone (DHA) is a three-carbon sugar that is the active ingredient in sunless tanning products and a by-product of electronic cigarette (e-cigarette) combustion. Increased use of sunless tanning products and e-cigarettes has elevated exposures to DHA through inhalation and absorption. Studies have confirmed that DHA is rapidly absorbed into cells and can enter into metabolic pathways following phosphorylation to dihydroxyacetone phosphate (DHAP), a product of fructose metabolism. Recent reports have suggested metabolic imbalance and cellular stress results from DHA exposures. However, the impact of elevated exposure to DHA on human health is currently under-investigated. We propose that exogenous exposures to DHA increase DHAP levels in cells and mimic fructose exposures to produce oxidative stress, mitochondrial dysfunction, and gene and protein expression changes. Here, we review cell line and animal model exposures to fructose to highlight similarities in the effects produced by exogenous exposures to DHA. Given the long-term health consequences of fructose exposure, this review emphasizes the pressing need to further examine DHA exposures from sunless tanning products and e-cigarettes.

Table of Contents

Dedication	iii
Acknowledgements	iv
Abstract	v
Table of Contents	vi
List of Figures	vii
List of Tables	viii
Introduction	ix
Fructose Exposures Generate Reactive Species	xii
Fructose Exposures Induce Mitochondrial Dysfunction	xvi
Fructose Exposure Causes Transcriptional Changes	xix
DHA Exposures Show Outcomes Similar to Fructose Exposures	xxiv
Discussion	xxviii
Conclusions	xxxii
References and Appendices	xxxiii

List of Figures

Fructolysis Pathway	xliv
Altered Expression of Proteins and Changes in Gene Expression Following Fructose and DHA Exposure	xlvi

List of Tables

Fructose Exposures in Cell Line Models	xlvii
Fructose Exposures in Animal Models	li
DHA Exposures Across Various Models	lv

Introduction

Dihydroxyacetone (DHA) is the simplest ketone sugar. When applied to the skin surface, it undergoes a Maillard reaction with the proteins to produce pigments called melanoidins. These melanoidins produce the browning effect associated with sunless tanning lotions. Tanning applications of DHA were discovered accidentally when DHA was tested as an alternative carbohydrate source to treat diabetes and other metabolic disorders (Wittgenstein and Berry, 1960; Martini, 2017). Browning of skin and gums were noted on patients administered DHA. DHA's topical use was quickly commercialized and received FDA approval for topical applications of up to 20% wt/vol in the late 1970s (FDA, 2002; FDA, 2015). Exposure estimates from a weekly topical application of a self-tanning lotion containing 10% DHA range from 0.91 mg/kg bw/week to 7.68 mg/kg bw/week, depending on absorption (SCCS, 2010).

More recently, DHA has also been found in the aerosols generated from electronic cigarettes (e-cigarettes). E-cigarettes use e-liquids containing propylene glycol and vegetable glycerin (glycerol) to mobilize flavorants and nicotine. Free radical oxidation of the e-liquids generates DHA with the amount of DHA generated depending on the device's combustion temperature (Vreeke et al., 2018). Exposure to DHA from e-cigarette vapor is estimated to be 0.5–2.33 µg/puff (Lee et al., 2018; Vreeke et al., 2018).

Sunless tanning exposures and the popularity of e-cigarettes have increased DHA concentrations to which humans are exposed (Pantini et al., 2007). Beyond skin absorption, DHA can be inhaled and absorbed through mucous membranes from e-cigarettes or the use of home or commercial spray tanning apparatuses. However, the systemic exposure effects of

DHA are poorly understood. Several recent studies have demonstrated the cytotoxicity and genotoxicity of DHA, but mechanisms underlying these outcomes are still being investigated.

Endogenously, the phosphorylated form of DHA, dihydroxyacetone phosphate (DHAP), is produced during glycolysis and fructolysis along with its isomer glyceraldehyde-3-phosphate (GAP; Figure 1) (Burch et al., 1970). When presented exogenously, DHA is rapidly absorbed into cells and is converted to DHAP by Triokinase/Flavin mononucleotide cyclase (TKFC, Figure 1), sometimes known as DHA kinase (DAK; Cabezas et al., 2005; Moreno et al., 2014; Marco-Rius et al., 2017). DHAP can integrate into nine different metabolic pathways (Burch et al., 1970; Moreno et al., 2014; Marco-Rius et al., 2017), either via glycerol-3-phosphate (G3P) following its reduction or via GAP following a thiamine diphosphate catalyzed isomerization (TPI, Figure 1).

High fructose diets lead to an increase in cellular DHAP and G3P levels, which are linked to increased formation of reactive oxygen and reactive nitrogen species (ROS/RNS), changes in metabolic profile, and reduced mitochondrial function (Gizak et al., 2019; Hernandez-Diazcouder et al., 2019; Taskinen et al., 2019). Elevated DHAP and G3P contribute to the development of insulin resistance associated with type 2 diabetes and advanced glycation end products (AGEs), which form when elevated levels of sugar metabolites react with proteins or lipids (Richard, 1993). These harmful compounds can react with amino, nucleic, and fatty acids to cause protein, DNA/RNA, and membrane damage (Yamagishi and Matsui, 2010; Fournet et al., 2018). Imbalances in DHAP and G3P due to elevated intracellular fructose levels also alter gene expression and create post-translational modifications that modulate enzyme activity, further hindering the efficiency of cellular metabolic pathways (Moraru et al., 2018).

Given that exogenous DHA exposure can also create imbalances in DHAP and G3P, examining fructose exposures may offer insight into the cellular consequences and mechanism underlying the cytotoxicity and genotoxicity of DHA. Here, we review in vitro and in vivo studies that examine fructose exposures to understand the emerging literature on DHA and contextualize the potential human health consequences of the exogenous DHA exposure.

Fructose Exposures Generate Reactive Species

It is well known that elevated cellular levels of reactive species increase oxidative stress within the cell and specific organelles. High levels of ROS/RNS can lead to intracellular damage of DNA and proteins inducing mutations and dysfunction. Within the mitochondria, increased levels of ROS and RNS have been shown to alter electron transport, reduce oxidative phosphorylation, reduce metabolic output, induce mitochondrial DNA (mtDNA) damage, and eventually trigger cell death (Indo et al., 2007).

Fructose exposures induce elevated reactive species formation by disrupting the balance between a cell's antioxidant defense mechanism and free radical concentration resulting in elevated oxidative stress (Touyz, 2012). ROS is produced as a natural consequence of flux through the fructolysis pathway, but increased flux can overwhelm the natural antioxidant balance allowing more reactive species to remain in the cell. ROS is also produced by fructose through the activation of NADPH oxidases (Delbosc et al., 2005). Interestingly, uric acid production also has a role in producing ROS following fructose exposure (Madlala et al., 2016). Increases in dietary fructose consumption promoted uric acid formation, which increased total cellular ROS via activation of transforming growth factor β 1 (TGF- β 1) and nicotinamide adenine dinucleotide phosphate (NADPH) oxidase 4 (Madlala et al., 2016).

ROS and RNS are induced by fructose exposure at both low (≤ 10 mM) and high (>10 mM) doses (Table 1). At 5 mM doses, the hepatocyte cell lines, rat hepatic parenchymal cells (RHPC), human hepatic (HLO2), and human hepatocellular carcinoma (HepG2) cells show elevated levels of hydrogen peroxide (H_2O_2), malondialdehyde (MDA), and nitric oxide

synthase (iNOS) for up to 48 hr (Zhang et al., 2015). Hepatic phagocytic Kupffer cells did not show any increase in total cellular ROS, H₂O₂, or MDA levels at 5 mM dosing, indicating metabolic differences between cell lines alter the generation of reactive species (Zhang et al., 2015).

At high fructose doses, L6 myotubes generated mitochondrial ROS within 1 hr and nitric oxide (NO) within 6 hr of 15 mM fructose treatment (Jaiswal et al., 2015a; Jaiswal et al., 2015b). iNOS also remained elevated for 48 hr indicating the prolonged presence of reactive species (Jaiswal et al., 2015a). While the human embryonic kidney (HEK293) cell line exposed to 30 mM fructose produced elevated total cellular ROS levels (Dornas et al., 2017), 15 mM fructose did not promote the generation of reactive oxygen species in dendritic cells. However, increased production of AGEs did occur (Jaiswal et al., 2019) in dendritic cells, emphasizing that fructose exposures induce reactive species in a cell-specific manner.

Systemic exposures to fructose also increased reactive species and oxidative damage at both low ($\leq 10\%$ dietary intake) and high doses ($> 10\%$ dietary intake) in animal models (Table 2). Dietary integration of 10% fructose led to the elevated generation of ROS and RNS across animal models. Sprague–Dawley rats exposed to 10% fructose dose for 8 weeks showed elevated total ROS, H₂O₂, MDA, xanthine oxidase, and iNOS, which all contributed to increases in hepatic oxidative stress (Zhang et al., 2015). A 12-week duration of the same dose in Wistar rats also resulted in high levels of total ROS generation in peripheral blood mononuclear cells but not in bone marrow mononuclear cells (Porto et al., 2015). Even C57BL/6 mice exposed to a 10% fructose dose over 20 weeks showed an 80% increase in total cellular ROS in cardiac tissue along with elevated mitochondrial H₂O₂ generation (Zhang et al.,

2016). These studies suggest that chronic exposure to low dose fructose increases total cellular reactive species in the liver and cardiac tissues.

As expected from the low dose fructose results, high fructose doses further increased intracellular ROS and oxidative stress. A 20% fructose diet increased oxidative stress levels in Fischer and Sprague–Dawley animal models for 20 weeks and during lactation/gestation periods, respectively (Dornas et al., 2017; Yamada et al., 2019). Hippocampal analysis of Sprague–Dawley rats demonstrated a 1.5-fold increase in total ROS due to increased fructose consumption (Yamada et al., 2019). Fischer rats treated with 20% fructose combined with 8% saline experienced hypertension, linking dysfunction to AGE formation and contractile changes in the vasculature (Dornas et al., 2017). High-dose fructose also elevated oxidative stress in response to increased 8-OHdG levels in Sprague–Dawley rats (Cioffi et al., 2017). Wistar rats exposed to a 60% fructose dose for 24 weeks showed elevated methylglyoxal and increased oxidative stress (Szucs et al., 2019). Of note, 60% fructose also elevated oxidative stress in Spontaneously Hypertensive rats, Wistar rats, and C57BL/6 mice (Cavarape et al., 2001; Mellor et al., 2010; Wu et al., 2017).

Current fructose exposure studies use various animal models and investigate multiple tissue types with little overlap between tissues studied and fructose dosing (Table 2). Of the studies discussed here, dietary supplementation of 7–10% and 60% fructose per day elevated reactive species formation in hepatic tissue of Sprague–Dawley rats and Wistar rats, respectively (Cavarape et al., 2001; Zhang et al., 2015; Cioffi et al., 2017). However, hepatic tissue from Wistar rats with 25% fructose administration exhibited no elevation in ROS levels (Garcia-Berumen et al., 2019; Yamada et al., 2019). Cardiac tissue showed increased ROS for C57BL/6

mice with 10% and 60% dietary fructose and Wistar rats given 60% fructose (Zhang et al., 2015; Szucs et al., 2019). Only limited analysis of kidney tissue was conducted with ROS formation observed after 20% fructose exposure in Fischer rat models (Dornas et al., 2017). Finally, Sprague–Dawley rats given a 20% fructose diet showed elevated ROS formation in hippocampal tissue, and Spontaneously Hypertensive rats administered a 60% fructose diet presented increased ROS in rostral ventrolateral medulla (RVLM) tissue (Wu et al., 2017; Yamada et al., 2019). While the models and dosing vary, these studies demonstrate excess fructose generates reactive species. However, dose-dependence and tissue-specificity cannot be inferred from the current literature.

Fructose Exposures Induce Mitochondrial Dysfunction

Fructose exposures also impact mitochondrial health by altering the metabolic output. Animal models show that fructose exposures impair insulin signaling pathways, reducing cellular glucose uptake and establishing a condition of chronic glucose intolerance (Tobey et al., 1982). Reductions in glucose uptake inhibit metabolic productivity exhibited by decreased oxygen consumption rate (OCR) and ATP content (Collins-Nakai et al., 1994). Current literature reveals that both low ($\leq 10\%$) and high fructose ($> 10\%$) supplementation induces mitochondrial dysfunction (Zhang et al., 2015; Jaiswal et al., 2015a; Jaiswal et al., 2015b).

In hepatoma FaO cells, 5.5 mM fructose alters mitochondrial respiration after 72 hr (Grasselli et al., 2019). In addition, 5 mM fructose alters mitochondrial membrane potential in RHPC, HLO2, and HepG2 liver cells (Zhang et al., 2015). High-dose fructose exposures increased mitochondrial membrane leakage, lowered mitochondrial membrane potential, and induced mitochondrial DNA damage in L6 myotubes (Jaiswal et al., 2015a). L6 myotubes also showed impaired insulin signaling, inhibited glucose uptake, and insulin resistance following 3 hr of the 15 mM fructose (Jaiswal et al., 2015b). Decreased rates of respiration were also observed in both dendritic cells and L6 myotubes after 15 mM fructose supplementation (Jaiswal et al., 2015a; Jaiswal et al., 2019). Moreover, high fructose exposure to L6 myotubes led to reduced rates of mitochondrial biogenesis and total cellular ATP production, contributing to a loss of metabolic function evident with a 30.5% reduction in ATP-related respiration (Jaiswal et al., 2015a).

Low dose fructose exposures to animal models have been linked to reduced rates of mitochondrial respiration, inhibited glucose uptake, and cofactor imbalances (Warren et al., 2014; Zhang et al., 2016). Low dose fructose intake for 20 weeks led to a 60% decrease in complex II respiratory activity and reduced oxygen consumption in States III and IV in C57BL/6 mice (Zhang et al., 2016). Similarly, analysis of Sprague–Dawley revealed reduced respiratory activity of complex I and II in the extensor digitorum longus (EDL) and soleus muscles, respectively; however, the respiratory activity of other complexes remained unchanged (Warren et al., 2014). Findings of reduced mitochondrial respiration correlate with reports of diminished ATP synthesis (Milakovic and Johnson, 2005).

Decreases in cellular glucose uptake for high-dose fructose supplementation to animal models leads to a decreased mitochondrial respiration (Table 2). Reduced glucose integration into metabolic pathways contributed to impaired mitochondrial function, as shown with high-dose fructose exposures to Sprague–Dawley and Wistar rats that exhibit decreased rates of respiration (Garcia-Berumen et al., 2019; Yamada et al., 2019).

High-dose fructose exposures in animal model studies have been capable of inducing elevated forms of oxidative damage evident through increased formation of nuclear and mtDNA lesions (Table 2). Fructose concentrations greater than 20% have produced oxidative mtDNA damage in the liver of Sprague–Dawley rats. In male Sprague–Dawley rats administered 30% of fructose per day, mtDNA copy number reduced by half, and there was a significant reduction in mitochondrial biogenesis, which decreased metabolic output (Cioffi et al., 2017). As shown by high-dose exposures to cell line models, fructose can institute mitochondrial impairment through changes in mitochondrial membrane potential (Table 1).

It should be noted that while fructose supplementation induced detrimental metabolic alterations such as reduced glucose uptake and insulin resistance in cell lines and animal models, human clinical trials do not show that fructose has a significant role in reducing metabolic health (Tappy and Le, 2012). However, there is evidence showing that diabetic patients exhibit elevated fructose concentrations in blood plasma (Kawasaki et al., 2002). Unfortunately, fructose plasma levels have not been measured in animal studies. More focus has been placed on plasma glucose and leptin measurements. Altogether, there is evidence that low- and high-dose fructose changes metabolism in cell lines and animals (Tables 1 & 2). More work is needed to understand how fructose effects in animal models translate into humans.

Fructose Exposure Causes Transcriptional Changes

Fructose exposures also induced unique transcriptional changes in response to elevated cellular stress, ROS, mitochondrial dysfunction, and cell death mechanisms (Figure 2). Oxidation of DNA and RNA by elevated ROS can disrupt replication, transcription and induce mutations within the genome (Poetsch, 2020). Oxidative DNA lesions can also act as transcription regulators through epigenetic or enhancer repressor activity to directly regulate gene expression (Ghosh and Mitchell, 1999; Pastukh et al., 2015; Fleming et al., 2017).

Low dose fructose altered Thioredoxin Interacting Protein (TXNIP) expression, associated with a cellular inflammatory signaling response to oxidative stress, in hepatocytes, RHPCs, HLO2s, and HepG2s cells (Zhang et al., 2015). Low dose fructose exposure also induced NLRP3 expression, which stimulates inflammasome formation and is linked to non-alcoholic fatty liver disease (NAFLD). Cultured hepatocytes (primary rat hepatocytes, RHPCs, HLO2, and HepG2 cells) treated with 5 mM fructose showed significant up-regulation of NLRP3 and inflammasome components Apoptosis-associated speck-like protein containing a CARD (ASC), Caspase-1, interleukin-1 β (IL-1 β), and IL-18 (Zhang et al., 2015). Low dose fructose exposures were also able to elevate fatty acid synthase (Fas) activity by 125% and MDA levels by 67% in primary hepatocytes (Grasselli et al., 2019). Elevated protein levels of signal transducer and activator of transcription 3 (STAT3) and suppressor of cytokine signaling-3 (SOCS3), which increase inflammatory cytokines, were also present in cultured HepG2 cells after low dose fructose exposures (Zhang et al., 2015). Even 550 μ M fructose caused a 3.5-fold increase in adipogenesis, indicated through overexpression of peroxisome proliferator-activated

receptor γ (Ppar γ) and Glucose transporter type 4 (GluT4) in 3 T3-L1 pre-adipocytes (Du and Heaney, 2012).

High-dose fructose exposures elevated iNOS, Nrf2, Jnk, Erk, Nf- κ b, and Mapk in response to oxidative stress in L6 myotubes (Jaiswal et al., 2015a; Jaiswal et al., 2015b). Human dendritic cells and HEK293 cells treated with high doses of fructose exhibited elevated expression of NF- κ B and its translocation to the nucleus (Dornas et al., 2017; Jaiswal et al., 2019). Human dendritic also showed increased expression of inflammasome proteins IL-1 β , IL-6, TNF- α , and IFN- γ at 24, 48, and 72 hr after high fructose exposure (Jaiswal et al., 2019). Dendritic cells also showed elevated apoptotic marker proteins and AGEs, which led to the activation of the receptor for advanced glycation end products (RAGE) (Jaiswal et al., 2019), consistent with Caspase-3, Caspase-7, and Caspase-9 activation in L6 myotubes (Jaiswal et al., 2015a).

Glucose exposure to animal models similarly showed elevated oxidative stress and induction of apoptosis (Piro et al., 2002). Glucose exposures disrupt cell metabolic pathways and lead to metabolic syndrome through signs of reduced glucose uptake and reduced OCR (Moreno-Fernández et al., 2018). Given that glucose and fructose can use similar metabolic pathways, it is not surprising that elevation in GLUT proteins was also observed. GLUT1 and GLUT4 participate in glucose uptake, while GLUT5 aids in fructose transport. Although there were no GluT4 and GluT5 mRNA expression changes for L6 myotubes treated with high-dose fructose, GluT4myc translocation to the cell surface was impaired upon fructose exposure (Jaiswal et al., 2019). GLUT1 expression increased in human dendritic cells exposed to 15 mM fructose (Jaiswal et al., 2019). 3 T3-L1 pre-adipocytes exhibited elevated levels of GluT5 expression at Days 4 and 6 following high fructose incubation, indicating that cellular activity became

altered as a function of fructose exposure, which suggests altered metabolic function (Du and Heaney, 2012; Legeza et al., 2014).

Low dose fructose exposures in animal models showed similar changes (Table 2). A 5% fructose dose with high-fat administered to Wistar rats produced elevated levels of Il-1 β , Il-6, and Nadph oxidase (Rosas-Villegas et al., 2017). Further, there were altered levels of catalase, glutathione peroxidase, glutathione reductase, and Sod1 due to exposure (Rosas-Villegas et al., 2017). Sprague–Dawley rat livers exhibited increased expression of Nlrp3 inflammation, Asc, Caspase-1, Il-1 β , and Il-18 after 10% fructose exposure (Zhang et al., 2015). Wistar male and female rats exposed to low dose fructose also showed elevated levels of inflammatory cytokines, Tnf- α , Il-1 β , Il-6, Il-10, and Il-18 expression in adipose tissues (Pektas et al., 2016). A 10% fructose dose in Wistar rats also showed increased expression of advanced oxidation protein products (AOPPs), apoptotic marker proteins, and inflammatory cytokines such as Il-12p70 and Il-6 (Porto et al., 2015). Elevated AGEs were also found in Wistar, Lewis, and hypertriglyceridic (HTG) rats administered with 10% fructose dose through increased post-translational pentosidine levels in rat aorta and skin tissue samples (Mikulikova et al., 2008).

Low dose fructose supplementation in C57BL/6 mice led to decreased cystic fibrosis transmembrane conductance regulator (CFTR) levels in cardiac tissue, contributing to heightened mitochondrial oxidative stress, impaired electron transport chain function, and induced myocardial hypertrophy (Zhang et al., 2016). Mitochondrial efficiency of Sprague–Dawley was also monitored through peroxisome proliferator-activated receptor- γ coactivator-1 α (Pgc-1 α) and Sirt3 protein expression levels after fructose exposure. There was a decrease in Pgc-1 α protein expression in both the EDL and soleus muscles of healthy rats with 10%

fructose exposure; however, there was an increase in Sirt3 expression in the soleus but a decline in the EDL muscle (Warren et al., 2014). Low dose exposures in Wistar male and female rats found elevated mRNA expression levels of insulin receptor β (Ir β), insulin receptor substrates (Irs-1, Irs-2), Akt, mTor, Pi3k, Ppary, Nrf2, and eNos, suggesting alterations in glucose uptake (Pektas et al., 2016).

High-dose fructose exposure to animal models similarly led to transcriptional changes due to alterations in oxidative stress and metabolic function upon supplementation (Table 2).

Spontaneously, hypertensive rats on a 60% fructose diet per day showed increased NADPH oxidase and suppression of extracellular SOD expression, contributing to elevated oxidative stress (Wu et al., 2017). A 20% fructose dose administered to Sprague–Dawley rats induced decreased lipid hydroperoxide (LPO) and increased 8-OHdG levels in the hippocampal region. Moreover, there was reduced expression levels of Ucp5, which is known to inhibit ROS formation with reduced mitochondrial Tfam gene expression levels (Yamada et al., 2019).

Fischer rats administered the same high-dose fructose over 20 weeks exhibited decreased renal SOD and catalase enzymatic expression (Dornas et al., 2017). C57BL/6 mice administered a 60% fructose dose experienced a non-significant increase of thioredoxin-2 (Thx2) gene expression levels (Mellor et al., 2010). Wistar rats administered 60% fructose had elevated expression of the elongation of very-long-chain fatty acids protein 6 (Elovl6) enzyme, which has an important role in NAFLD by transforming C16 saturated and monounsaturated fatty acids into C18 compounds (Szucs et al., 2019).

There are indications that high-dose fructose supplementation to animal models has differing effects on apoptosis triggering pathways (Table 2). High fructose exposed Wistar rats had

decreased catalase mRNA expression in the liver, heart, skeletal muscle, and adipose tissue, which is pro-apoptotic (Cavarape et al., 2001). There were also increased levels of creatine kinase (CK), CK-MB, and lactate dehydrogenase (LDH), which are indicative of myocardial injury (Szucs et al., 2019). However, a separate Wistar rat study found no change in caspase-7 and Bax expression upon treatment; however, there was an increase in anti-apoptotic 3-ketoacyl-CoA thiolase in mitochondria of cardiac tissue, which diminished Bnip3-induced apoptosis (Szucs et al., 2019).

Both cell line and animal model studies show fructose induces transcriptional changes and apoptosis (Tables 1 & 2). There are clear links between the elevated reactive species and these outcomes, suggesting that fructose exposure does have a significant role in toxicity (Porto et al., 2015; Zhang et al., 2015; Jaiswal et al., 2015a).

DHA Exposures Show Outcomes Similar to Fructose Exposures

Early toxicological investigations found DHA to be mutagenic in *Salmonella typhimurium* strain TA100 with and without metabolic activation (Table 3) (Pham et al., 1979).

Mutagenicity of DHA is not surprising given that glucose, fructose, and galactose are mutagenic (Brands et al., 2000). Interestingly, ketose sugars like fructose are more mutagenic than glucose and galactose, and higher mutagenic activity corresponds with a higher Maillard reactivity (Brands et al., 2000; Laroque et al., 2008). DHA is a ketose, precursor to ribose, the most reactive sugar in modifying proteins by the Maillard reaction.

Low millimolar doses of DHA are cytotoxic and genotoxic in immortalized keratinocytes, melanoma cells, human embryonic kidney cells, and reconstructed epidermis (Table 3) (Petersen et al., 2004; Smith et al., 2018; Smith et al., 2019; Perer et al., 2020). Genotoxicity of fructose has been previously described and attributed to the generation of genotoxic metabolites like reactive species (ROS/RNS) and glyoxal (Table 1) (Hansen et al., 2008). Similarly, the genotoxicity of DHA involves the generation of reactive species and induction of strand breaks. ROS was generated after 5 mM exposures to DHA in A375P cells (Smith et al., 2018). ROS was also observed in the immortalized keratinocyte cell line HaCaT after 25 and 50 mM doses (Perer et al., 2020). Increases in ROS were also observed when ex vivo skin was exposed to DHA then exposed to ultraviolet (UV) light (Jung et al., 2008). Strand breaks and replication stress were also observed in HaCaT and A375P cells through comet assay and γ H2AX foci formation (Petersen et al., 2004; Smith et al., 2018; Perer et al., 2020). HEK293T cells did not show increases in ROS, but changes in NAD(P)H and GSH/GSSG levels indicate the presence of reactive species after 5 mM DHA exposure (Smith et al., 2019).

Both fructose and DHA exposures increase reactive species content in cell models. However, fructose investigations infer that the formation of these species can lead to detrimental cellular effects such as metabolic dysfunction, and evidence is only emerging that DHA exposures cause these outcomes as well (Table 1). It is currently unknown if ROS formation following DHA exposure can be driven by uric acid. Elevated ROS formation for both fructose and DHA investigations are similar in that they are dependent on the activation of NADPH oxidases by AGEs, which contribute to elevated oxidative stress (Wautier et al., 2001; Kuroda et al., 2010).

Fructose cytotoxicity is less well described independent of other stressors, but 12 mM fructose was 50% cytotoxic to primary hepatocytes (Lee et al., 2009). Recent characterization of DHA demonstrates higher genotoxicity and cytotoxicity than is associated with fructose exposures, indicating the metabolic mechanisms to deal with excess fructose are more robust than those that deal with an excess of 3-carbon metabolites. The metabolic dependence of DHA cytotoxicity is supported by variations in DHA sensitivity and the mechanisms of cell death between cell lines. Petersen et al. and Perer et al. report cytotoxic doses for the immortalized keratinocyte cell lines HaCaT at 25 mM, while A375P melanoma cells and HEK293T cells show more sensitivity with IC90 doses of 5 mM (Petersen et al., 2004; Smith et al., 2018; Smith et al., 2019; Perer et al., 2020). The different cell line models had varied cell death mechanisms from apoptosis (HaCaT and A375P) to autophagy (HEK293T) (Petersen et al., 2003; Smith et al., 2018; Smith et al., 2019; Perer et al., 2020). A brief period of senescence was even observed in the A375P melanoma cells exposed to 5 mM DHA (Smith et al., 2018), supporting metabolic dependence for the cytotoxic effects and likely the genotoxic effects.

Work with hyperpolarized DHA injected into C57BL/6 mice and Sprague–Dawley rats demonstrated generation of different metabolites after DHA exposures in the liver and kidney (Moreno et al., 2014; Marco-Rius et al., 2017). These works focused on using the hyperpolarized DHA as a metabolic probe, so high millimolar doses and short exposure time points were used (Table 3). These data confirm DHA is rapidly absorbed by tissues and incorporated into metabolic pathways. Critically, the rates of incorporation were dependent on the fed state of the animal (Moreno et al., 2014). Additionally, conversion of DHA to DHAP by TKFC seems to be a rate-limiting step for metabolic incorporation, with higher levels of DHA seen in the kidney than in the liver (Marco-Rius et al., 2017). TKFC expression varies across tissues, and mutations in TKFC are observed in individuals with metabolic disorders (Uhlen et al., 2015; Uhlen et al., 2017; Wortmann et al., 2020).

Once incorporated into metabolic pathways, DHA and DHAP can induce AGE formation, damaging proteins and lipids, similar to fructose exposures. Perer et al. demonstrated that DHA-derived AGEs could be measured in immortalized keratinocytes, human epidermal constructs, and mouse skin (Perer et al., 2020). This is consistent with observed AGE formation in fructose exposure studies; however, DHA is a more efficient glycation agent (Seneviratne et al., 2012). Perer et al. also showed that non-cytotoxic doses of DHA activated stress-related signal transduction pathways (p-p38, p-Hsp27[S15/S78], p-eIF2 α) in immortalized keratinocytes (Perer et al., 2020). Elevated levels of stress response genes HSPA1A, HSPA6, HSPD1, IL6, and DDIT3, were also observed in both cell culture and reconstructed skin (Figure 2) (Perer et al., 2020).

Along with AGEs and stress responses, DHA exposures altered mitochondrial function and impacted NAD(P)H pools (Smith et al., 2018; Smith et al., 2019). Similar to low dose fructose exposures, DHA reduced ATP production and respiration rates in HEK293T cells (Smith et al., 2019). Fructose exposures also showed reductions in mtDNA, mitochondrial biogenesis, and respiratory activity (Tables 1 and 2). These findings within fructose literature provide insight into the potential metabolic consequences of DHA exposure. The NAD(P)H pool imbalance likely impacts the efficiency of complex I to alter mitochondrial function. Still, a more in-depth analysis of the mitochondrial impact of DHA is needed to clarify the mechanisms underlying mitochondrial dysfunction.

Discussion

While studies to date have focused on more acute DHA exposures (Table 3), the data from these studies indicate the DHA exposures have metabolic, cytotoxic, and genotoxic outcomes that are strikingly similar to fructose exposures but occur at much lower doses than fructose (Gizak et al., 2019; Hernandez-Diazcouder et al., 2019; Taskinen et al., 2019). These similarities are not surprising, given DHAP is generated from the breakdown of fructose. However, DHAP from fructose exposures is generated in equilibrium with G3P. DHA generates DHAP dependent on TKFC activity within each cell or tissue and produces an imbalance in 3-carbon metabolites uniquely in each tissue.

Imbalance in DHAP and G3P has been linked with anemia, neurological disorders, diabetes, and cancer (Orosz et al., 2009; Kitada et al., 2010; Rabbani et al., 2016). Imbalance in this pathway is most often seen when defects in triosephosphate isomerase (TPI), which interconverts G3P and DHAP, results in the accumulation of DHAP. Excess DHAP is proposed to be converted to methylglyoxal and other AGEs, damaging DNA and proteins within the cell and causing neurological disorders and early childhood death, even though energy metabolism is unaffected (Li et al., 2008; Orosz et al., 2009).

Conversion of exogenous DHA to DHAP should cause a brief imbalance of DHAP/G3P, which the cell can re-equilibrate through multiple enzymatic reactions. However, the studies examining DHA exposure reviewed here show more acute genotoxic, metabolic, and cytotoxic outcomes than expected from equivalent fructose exposures (Tables 1 and 2). This suggests excess DHA and TKFC-converted DHAP are not readily metabolically incorporated for

equilibration, or if equilibration occurs, it comes at a price to the cell health. DHA that is not readily converted into DHAP may induce unique protein and DNA damage that has yet to be characterized. More work is needed to understand the fate and impact of DHA that is not converted to DHAP in cells.

The DHA converted to DHAP accumulates endogenous toxins like ROS, RNS, and AGEs that damage DNA and proteins within cells. Therefore, the wealth of fructose studies already in the literature provide critical insight into the potential exposure effects of systemic DHA, which could place significant stress on cellular reduction and oxidation pathways, mitochondrial function, and metabolism (Tables 1 and 2). More importantly, it also highlights unexplored areas of systemic DHA exposures where inflammatory cytokines and inflammasome proteins are up-regulated. Chronic, long-term DHA exposure may act similarly to high fructose diets and induce metabolic reprogramming that reduces glucose uptake, changes glucose tolerance, and alters metabolic dependence of tissues. This type of metabolic reprogramming is important in the pathogenesis of obesity and diabetes.

Additionally, DHAP resulting from DHA exposure could impair lipid metabolism, like fructose exposures, and contribute to increased adipose tissue, higher body weights, blood pressures, and plasma triglyceride concentrations in exposed individuals. These types of outcomes from DHA exposure could impact the development of chronic illnesses like insulin resistance and NAFLD. More work is needed with animals exposed to DHA under different dietary conditions to understand the consequences of exposure across different tissue types.

Critically, work characterizing fructose exposures also demonstrates that other underlying metabolic factors, like high-fat diets, can alter the cellular consequences of DHA exposure. Co-exposure of fructose with a high-fat diet showed more elevated ROS generation alongside increased levels of MDA, H₂O₂, and oxidative damage in adipose, liver, skeletal, and kidney tissue types at lower fructose doses (Rosas-Villegas et al., 2017). The interaction of DHA or TKFC-converted DHAP with these underlying metabolic conditions could further exacerbate the reactive species generated and the genotoxicity and cytotoxicity of DHA.

One other possibility is that low dose exposures to fructose or DHA could stimulate antioxidant mechanisms and transcription factors like NF- κ B to reduce reactive species (Figure 2). As noted in some fructose studies, enzymes that scavenge reactive species are up-regulated and could provide a beneficial cellular effect by reducing reactive species and promoting the degradation of damaged proteins. However, there are insufficient studies of low dose DHA exposure to understand if there is a beneficial vs. adverse dose threshold. More studies, including both high and low doses of DHA, would offer new insight into the cell's ability to use DHA as a carbon source and identify where chronic or acute exposure effects occur.

Evidence that exogenous DHA exposures contribute to disease states is currently lacking. However, there is ample evidence in the literature that imbalances in DHAP and G3P from fructose exposures, diabetes, and other disease states induce protein and DNA damage, metabolic reprogramming and contribute to disease progression. Significantly, more work is needed both in vitro and in vivo to understand the consequences of acute and chronic exposures to exogenous DHA. Given that DHA exposures are following an increasing trend, the wealth of fructose data already in the literature offers a unique opportunity to investigate the differences

between fructose and DHA exposures. Fructose studies also provide comparison points for examining the health consequences of DHA and TKFC-converted DHAP exposures.

Conclusions

Exogenous exposures to DHA can occur through the use of sunless tanning products and e-cigarettes. Exposures to millimolar doses of DHA are genotoxic, cytotoxic, and induce metabolic reprogramming. Comparison with existing fructose exposure literature highlights that both fructose and DHA elevate oxidative stress due to the generation of reactive species. Both agents also induce mitochondrial changes that decreased overall function. The fructose data suggests these changes occur through alter electron transport and through the induction of DNA damage. These mechanisms need to be confirmed in DHA exposed models.

Additionally, gene expression changes observed in both fructose and DHA exposure models confirm the induction of cellular stress, even at non-cytotoxic doses that may induce metabolic reprogramming. In summary, DHA exposures are similar to fructose exposure, but they cause detrimental cellular consequences more rapidly and at lower doses. Therefore, fructose exposures can help develop a framework for investigating the health effects of DHA exposures and provide a better understanding of the potential health consequences for exposed individuals.

References

1. Brands, C.M., Alink, G.M., van Boekel, M.A. and Jongen, W.M. (2000) Mutagenicity of heated sugar-casein systems: Effect of the Maillard reaction. *Journal of Agricultural and Food Chemistry*, 48(6), 2271–2275.
2. Burch, H.B., Lowry, O.H., Meinhardt, L., Max, P., Jr. and Chyu, K. (1970) Effect of fructose, dihydroxyacetone, glycerol, and glucose on metabolites and related compounds in liver and kidney. *Journal of Biological Chemistry*, 245(8), 2092–2102.
3. Cabezas, A., Costas, M.J., Pinto, R.M., Couto, A. and Cameselle, J.C. (2005) Identification of human and rat FAD-AMP lyase (cyclic FMN forming) as ATP-dependent dihydroxyacetone kinases. *Biochemical and Biophysical Research Communications*, 338(4), 1682–1689.
4. Cavarape, A., Feletto, F., Mercuri, F., Quagliaro, L., Daman, G. and Ceriello, A. (2001) High-fructose diet decreases catalase mRNA levels in rat tissues. *Journal of Endocrinological Investigation*, 24(11), 838–845.
5. Cioffi, F., Senese, R., Lasala, P., Ziello, A., Mazzoli, A., Crescenzo, R., Liverini, G., Lanni, A., Goglia, F., and Iossa, S. (2017) Fructose-Rich Diet Affects Mitochondrial DNA Damage and Repair in Rats. *Nutrients*, 9 (4), 323.
6. Collins-Nakai, R.L., Noseworthy, D. and Lopaschuk, G.D. (1994) Epinephrine increases ATP production in hearts by preferentially increasing glucose metabolism. *American Journal of Physiology*, 267(5 Pt 2), H1862–H1871.
7. Delbosc, S., Paizanis, E., Magous, R., Araiz, C., Dimo, T., Cristol, J.P., Cros, G. and Azay, J. (2005) Involvement of oxidative stress and NADPH oxidase activation in the

- development of cardiovascular complications in a model of insulin resistance, the fructose-fed rat. *Atherosclerosis*, 179(1), 43–49.
8. Dornas, W.C., Cardoso, L.M., Silva, M., Machado, N.L., Chianca, D.A., Jr., Alzamora, A.C., Lima, W.G., Lagente, V. and Silva, M.E. (2017) Oxidative stress causes hypertension and activation of nuclear factor-kappaB after high-fructose and salt treatments. *Scientific Reports*, 7, 46051.
 9. Du, L. and Heaney, A.P. (2012) Regulation of adipose differentiation by fructose and GluT5. *Molecular Endocrinology*, 26(10), 1773–1782.
 10. FDA. (2002) Code of Federal Regulations, title 21. Washington, D.C.: U.S. Food and Drug Administration, p. 1150.
 11. FDA. (2015) Sunless Tanners & Bronzers. Washington, D.C.: U.S. Food and Drug Administration.
 12. Fleming, A.M., Ding, Y. and Burrows, C.J. (2017) Oxidative DNA damage is epigenetic by regulating gene transcription via base excision repair. *Proceedings of the National Academy of Sciences of the United States of America*, 114(10), 2604–2609.
 13. Fournet, M., Bonte, F. and Desmouliere, A. (2018) Glycation damage: A possible hub for major pathophysiological disorders and aging. *Aging & Disease*, 9(5), 880–900.
 14. Garcia-Berumen CI, Ortiz-Avila O, Vargas-Vargas MA, Del Rosario-Tamayo BA, Guajardo-Lopez C, Saavedra-Molina A, Rodriguez-Orozco AR, Cortes-Rojo C. 2019. The severity of rat liver injury by fructose and high fat depends on the degree of respiratory dysfunction and oxidative stress induced in mitochondria. *Lipids in Health and Disease* 18(1):78.
 15. Ghosh, R. and Mitchell, D.L. (1999) Effect of oxidative DNA damage in promoter elements on transcription factor binding. *Nucleic Acids Research*, 27(15), 3213–3218.

16. Gizak, A., Duda, P., Wisniewski, J. and Rakus, D. (2019) Fructose-1,6-bisphosphatase: From a glucose metabolism enzyme to multifaceted regulator of a cell fate. *Advances in Biological Regulation*, 72, 41–50.
17. Grasselli, E., Baldini, F., Vecchione, G., Oliveira, P.J., Sardao, V.A., Voci, A., Portincasa, P. and Vergani, L. (2019) Excess fructose and fatty acids trigger a model of nonalcoholic fatty liver disease progression in vitro: Protective effect of the flavonoid silybin. *International Journal of Molecular Medicine*, 44(2), 705–712.
18. Hansen, M., Baunsgaard, D., Autrup, H., Vogel, U.B., Moller, P., Lindecrona, R., Wallin, H., Poulsen, H.E., Loft, S. and Dragsted, L.O. (2008) Sucrose, glucose and fructose have similar genotoxicity in the rat colon and affect the metabolome. *Food and Chemical Toxicology*, 46 (2), 752–760.
19. Hernández-Díazcouder, A., Romero-Nava, R., Carbó, R., SánchezLozada, L.G., and Sánchez-Muñoz, F. (2019) High Fructose Intake and Adipogenesis. *International Journal of Molecular Sciences*, 20(11), 2787.
20. Indo, H.P., Davidson, M., Yen, H.C., Suenaga, S., Tomita, K., Nishii, T., Higuchi, M., Koga, Y., Ozawa, T. and Majima, H.J. (2007) Evidence of ROS generation by mitochondria in cells with impaired electron transport chain and mitochondrial DNA damage. *Mitochondrion*, 7(1–2), 106–118
21. Jaiswal N., Agrawal S., Agrawal A. (2019) High fructose-induced metabolic changes enhance inflammation in human dendritic cells. *Clinical & Experimental Immunology*, 197(2), 237–249.
22. Jaiswal, N., Maurya, C.K., Arha, D., Avisetti, D.R., Prathapan, A., Raj, P.S., Raghu, K.G., Kalivendi, S.V. and Tamrakar, A.K. (2015a) Fructose induces mitochondrial

- dysfunction and triggers apoptosis in skeletal muscle cells by provoking oxidative stress. *Apoptosis*, 20(7), 930–947.
23. Jaiswal, N., Maurya, C.K., Pandey, J., Rai, A.K. and Tamrakar, A.K. (2015b) Fructose-induced ROS generation impairs glucose utilization in L6 skeletal muscle cells. *Free Radical Research*, 49(9), 1055–1068.
24. Jung, K., Seifert, M., Herrling, Th., and Fuchs, J. (2008) UV-generated free radicals (FR) in skin: Their prevention by sunscreens and their induction by self-tanning agents. *Spectrochimica Acta Part A: Molecular and Biomolecular Spectroscopy*, 69(5), 1423–1428.
25. Kawasaki, T., Akanuma, H. and Yamanouchi, T. (2002) Increased fructose concentrations in blood and urine in patients with diabetes. *Diabetes Care*, 25(2), 353–357.
26. Kitada, M., Zhang, Z., Mima, A. and King, G.L. (2010) Molecular mechanisms of diabetic vascular complications. *Journal of Diabetes Investigation*, 1(3), 77–89.
27. Kuroda, J., Ago, T., Matsushima, S., Zhai, P., Schneider, M.D. and Sadoshima, J. (2010) NADPH oxidase 4 (Nox4) is a major source of oxidative stress in the failing heart. *Proceedings of the National Academy of Sciences of the United States of America*, 107(35), 15565–15570.
28. Laroque, D., Inisan, C., Berger, C., Vouland, É., Dufossé, L. and Guérard, F. (2008) Kinetic study on the Maillard reaction. Consideration of sugar reactivity. *Food Chemistry*, 111(4), 1032–1042.
29. Lee, O., Bruce, W.R., Dong, Q., Bruce, J., Mehta, R. and O'Brien, P.J. (2009) Fructose and carbonyl metabolites as endogenous toxins. *ChemicoBiological Interactions*, 178(1–3), 332–339.

30. Lee, Y.O., Nonnemaker, J.M., Bradfield, B., Hensel, E.C. and Robinson, R.J. (2018) Examining daily electronic cigarette puff topography among established and nonestablished cigarette smokers in their natural environment. *Nicotine & Tobacco Research*, 20(10), 1283–1288.
31. Legeza, B., Balazs, Z. and Odermatt, A. (2014) Fructose promotes the differentiation of 3T3-L1 adipocytes and accelerates lipid metabolism. *FEBS Letters*, 588(3), 490–496.
32. Li, Y., Cohenford, M.A., Dutta, U. and Dain, J.A. (2008) In vitro nonenzymatic glycation of guanosine 50 -triphosphate by dihydroxyacetone phosphate. *Analytical and Bioanalytical Chemistry*, 392(6), 1189–1196.
33. Madlala, H.P., Maarman, G.J. and Ojuka, E. (2016) Uric acid and transforming growth factor in fructose-induced production of reactive oxygen species in skeletal muscle. *Nutrition Reviews*, 74(4), 259–266.
34. Marco-Rius, I., von Morze, C., Sriram, R., Cao, P., Chang, G.Y., Milshteyn, E., Bok, R.A., Ohliger, M.A., Pearce, D., Kurhanewicz, J., Larson, P.E., Vigneron, D.B. and Merritt, M. (2017) Monitoring acute metabolic changes in the liver and kidneys induced by fructose and glucose using hyperpolarized [2-13 C]dihydroxyacetone. *Magnetic Resonance in Medicine*, 77(1), 65–73.
35. Martini, M.C. (2017) Self-tanning and sunless tanning products. *Annals of Dermatology and Venereology*, 144(10), 638–644.
36. Mellor, K., Ritchie, R.H., Meredith, G., Woodman, O.L., Morris, M.J. and Delbridge, L.M. (2010) High-fructose diet elevates myocardial superoxide generation in mice in the absence of cardiac hypertrophy. *Nutrition*, 26(7–8), 842–848.

37. Mikulikova, K., Eckhardt, A., Kunes, J., Zicha, J. and Miksik, I. (2008) Advanced glycation end-product pentosidine accumulates in various tissues of rats with high fructose intake. *Physiological Research*, 57(1), 89–94.
38. Milakovic, T. and Johnson, G.V. (2005) Mitochondrial respiration and ATP production are significantly impaired in striatal cells expressing mutant huntingtin. *Journal of Biological Chemistry*, 280(35), 30773–30782.
39. Moraru, A., Wiederstein, J., Pfaff, D., Fleming, T., Miller, A.K., Nawroth, P. and Teleanu, A.A. (2018) Elevated levels of the reactive metabolite Methylglyoxal recapitulate progression of type 2 diabetes. *Cell Metabolism*.
40. Moreno, K.X., Satapati, S., DeBerardinis, R.J., Burgess, S.C., Malloy, C.R. and Merritt, M.E. (2014) Real-time detection of hepatic gluconeogenic and glycogenolytic states using hyperpolarized [2-13C]dihydroxyacetone. *Journal of Biological Chemistry*, 289(52), 35859–35867.
41. Moreno-Fernández, S., Garcés-Rimón, M., Vera, G., Astier, J., Landrier, J., and Miguel, M. (2018) High Fat/High Glucose Diet Induces Metabolic Syndrome in an Experimental Rat Model. *Nutrients*, 10(10), 1502.
42. Orosz, F., Olah, J. and Ovadi, J. (2009) Triosephosphate isomerase deficiency: New insights into an enigmatic disease. *Biochimica et Biophysica Acta*, 1792(12), 1168–1174.
43. Pantini, G., Ingoglia, R., Brunetta, F. and Brunetta, A. (2007) Sunless tanning products containing dihydroxyacetone in combination with a perfluoropolyether phosphate. *International Journal of Cosmetic Science*, 29(3), 201–209.
44. Pastukh, V., Roberts, J.T., Clark, D.W., Bardwell, G.C., Patel, M., AlMehdi, A.B., Borchert, G.M. and Gillespie, M.N. (2015) An oxidative DNA "damage" and repair

- mechanism localized in the VEGF promoter is important for hypoxia-induced VEGF mRNA expression. *American Journal of Physiology-Lung Cellular and Molecular Physiology*, 309(11), L1367–L1375.
45. Pektas, M.B., Koca, H.B., Sadi, G. and Akar, F. (2016) Dietary fructose activates insulin signaling and inflammation in adipose tissue: Modulatory role of resveratrol. *BioMed Research International*, 2016, 8014252.
46. Perer, J., Jandova, J., Fimbres, J., Jennings, E.Q., Galligan, J.J., Hua, A. and Wondrak, G.T. (2020) The sunless tanning agent dihydroxyacetone induces stress response gene expression and signaling in cultured human keratinocytes and reconstructed epidermis. *Redox Biology*, 36, 101594.
47. Petersen, A.B., Na, R. and Wulf, H.C. (2003) Sunless skin tanning with dihydroxyacetone delays broad-spectrum ultraviolet photocarcinogenesis in hairless mice. *Mutation Research*, 542(1–2), 129–138.
48. Petersen, A.B., Wulf, H.C., Gniadecki, R. and Gajkowska, B. (2004) Dihydroxyacetone, the active browning ingredient in sunless tanning lotions, induces DNA damage, cell-cycle block and apoptosis in cultured HaCaT keratinocytes. *Mutation Research*, 560(2), 173–186.
49. Pham, H.N., DeMarini, D.M. and Brockmann, H.E. (1979) Mutagenicity of skin tanning lotions. *Journal of Environmental Pathology and Toxicology*, 3(1–2), 227–231.
50. Piro, S., Anello, M., Di Pietro, C., Lizzio, M.N., Patane, G., Rabuazzo, A.M., Vigneri, R., Purrello, M. and Purrello, F. (2002) Chronic exposure to free fatty acids or high glucose induces apoptosis in rat pancreatic islets: Possible role of oxidative stress. *Metabolism*, 51(10), 1340–1347.

51. Poetsch, A.R. (2020) The genomics of oxidative DNA damage, repair, and resulting mutagenesis. *Computational and Structural Biotechnology Journal*, 18, 207–219.
52. Porto, M.L., Lirio, L.M., Dias, A.T., Batista, A.T., Campagnaro, B.P., Mill, J. G., Meyrelles, S.S. and Baldo, M.P. (2015) Increased oxidative stress and apoptosis in peripheral blood mononuclear cells of fructose-fed rats. *Toxicology In Vitro*, 29(8), 1977–1981.
53. Rabbani, N., Xue, M. and Thornalley, P.J. (2016) Methylglyoxal-induced dicarbonyl stress in aging and disease: First steps towards glyoxalase 1-based treatments. *Clinical Science (London)*, 130(19), 1677–1696.
54. Richard, J.P. (1993) Mechanism for the formation of methylglyoxal from triosephosphates. *Biochemical Society Transactions*, 21(2), 549–553.
55. Rosas-Villegas A., Sánchez-Tapia, M., Avila-Nava, A., Ramírez V., Tovar A., and Torres N. (2017) Differential Effect of Sucrose and Fructose in Combination with a High Fat Diet on Intestinal Microbiota and Kidney Oxidative Stress. *Nutrients*, 9(4), 393.
56. SCCS. (2010) Opinion on dihydroxyacetone. Brussels: Scientific Committee on Consumer Safety.
57. Seneviratne, C., Dombi, G.W., Liu, W., and Dain, J.A. (2012) In vitro glycation of human serum albumin by dihydroxyacetone and dihydroxyacetone phosphate. *Biochemical and Biophysical Research Communications*, 417(2), 817–823.
58. Smith, K.R., Granberry, M., Tan, M.C.B., Daniel, C.L. and Gassman, N.R. (2018) Dihydroxyacetone induces G2/M arrest and apoptotic cell death in A375P melanoma cells. *Environmental Toxicology*, 33(3), 333–342.

59. Smith, K.R., Hayat, F., Andrews, J.F., Migaud, M.E. and Gassman, N.R. (2019) Dihydroxyacetone exposure alters NAD(P)H and induces mitochondrial stress and autophagy in HEK293T cells. *Chemical Research in Toxicology*, 32(8), 1722–1731.
60. Szucs, G., Soja, A., Peter, M., Sarkozy, M., Bruszel, B., Siska, A., Foldesi, I., Szabo, Z., Janaky, T., Vigh, L., Balogh, G. and Csont, T. (2019) Prediabetes induced by fructose-enriched diet influences cardiac Lipidome and proteome and leads to deterioration of cardiac function prior to the development of excessive oxidative stress and cell damage. *Oxidative Medicine and Cellular Longevity*, 2019, 3218275.
61. Tappy, L. and Le, K.A. (2012) Does fructose consumption contribute to non-alcoholic fatty liver disease? *Clinics and Research in Hepatology and Gastroenterology*, 36(6), 554–560.
62. Taskinen, Packard, Borén (2019) Dietary Fructose and the Metabolic Syndrome. *Nutrients*, 11(9), 1987.
63. Tobey, T.A., Mondon, C.E., Zavaroni, I. and Reaven, G.M. (1982) Mechanism of insulin resistance in fructose-fed rats. *Metabolism*, 31(6), 608–612.
64. Touyz, R.M. (2012) Chapter 69—Reactive oxygen species and oxidative stress. In: Robertson, D., Biaggioni, I., Burnstock, G., Low, P.A. and Paton, J.F.R. (Eds.) *Primer on the autonomic nervous system*, 3rd edition. San Diego: Academic Press, pp. 335–338.
65. Uhlen, M., Fagerberg, L., Hallstrom, B.M., Lindskog, C., Oksvold, P., Mardinoglu, A., Sivertsson, A., Kampf, C., Sjostedt, E., Asplund, A., Olsson, I., Edlund, K., Lundberg, E., Navani, S., Szigartyo, C.A., Odeberg, J., Djureinovic, D., Takanen, J.O., Hober, S., Alm, T., Edqvist, P.H., Berling, H., Tegel, H., Mulder, J., Rockberg, J., Nilsson, P., Schwenk, J.M., Hamsten, M., von Feilitzen, K., Forsberg, M., Persson, L., Johansson,

- F., Zwahlen, M., von Heijne, G., Nielsen, J. and Ponten, F. (2015) Proteomics. Tissue-based map of the human proteome. *Science*, 347(6220), 1260419.
66. Uhlen, M., Zhang, C., Lee, S., Sjostedt, E., Fagerberg, L., Bidkhori, G., Benfeitas, R., Arif, M., Liu, Z., Edfors, F., Sanli, K., von Feilitzen, K., Oksvold, P., Lundberg, E., Hober, S., Nilsson, P., Mattsson, J., Schwenk, J.M., Brunnstrom, H., Glimelius, B., Sjoblom, T., Edqvist, P.H., Djureinovic, D., Micke, P., Lindskog, C., Mardinoglu, A. and Ponten, F. (2017) A pathology atlas of the human cancer transcriptome. *Science*, 357(6352), eaan2507.
67. Vreeke, S., Korzun, T., Luo, W., Jensen, R.P., Peyton, D.H. and Strongin, R. M. (2018) Dihydroxyacetone levels in electronic cigarettes: Wick temperature and toxin formation. *Aerosol Science and Technology*, 52(4), 370–376.
68. Warren, B.E., Lou, P.H., Lucchinetti, E., Zhang, L., Clanachan, A.S., Affolter, A., Hersberger, M., Zaugg, M. and Lemieux, H. (2014) Early mitochondrial dysfunction in glycolytic muscle, but not oxidative muscle, of the fructose-fed insulin-resistant rat. *American Journal of Physiology-Endocrinology and Metabolism*, 306(6), E658–E667.
69. Wautier, M.P., Chappey, O., Corda, S., Stern, D.M., Schmidt, A.M. and Wautier, J.L. (2001) Activation of NADPH oxidase by AGE links oxidant stress to altered gene expression via RAGE. *American Journal of Physiology-Endocrinology and Metabolism*, 280(5), E685–E694.
70. Wittgenstein, E. and Berry, H.K. (1960) Staining of skin with dihydroxyacetone. *Science*, 132(3431), 894–895.
71. Wortmann, S.B., Meunier, B., Mestek-Boukhibar, L., van den Broek, F., Maldonado, E.M., Clement, E., Weghuber, D., Spenger, J., Jaros, Z., Taha, F., Yue, W.W., Heales, S.J., Davison, J.E., Mayr, J.A. and Rahman, S. (2020) Bi-allelic variants in TKFC

- encoding triokinase/FMN cyclase are associated with cataracts and multisystem disease. *American Journal of Human Genetics*, 106(2), 256–263.
72. Wu, K.L., Wu, C.W., Tain, Y.L., Chao, Y.M., Hung, C.Y., Tsai, P.C., Wang, W. S. and Shih, C.D. (2017) Effects of high fructose intake on the development of hypertension in the spontaneously hypertensive rats: The role of AT1R/gp91(PHOX) signaling in the rostral ventrolateral medulla. *Journal of Nutritional Biochemistry*, 41, 73–83.
73. Yamada, H., Munetsuna, E., Yamazaki, M., Mizuno, G., Sadamoto, N., Ando, Y., Fujii, R., Shiogama, K., Ishikawa, H., Suzuki, K., Shimono, Y., Ohashi, K. and Hashimoto, S. (2019) Maternal fructose-induced oxidative stress occurs via Tfam and Ucp5 epigenetic regulation in offspring hippocampi. *FASEB Journal*, 33(10), 11431–11442.
74. Yamagishi, S. and Matsui, T. (2010) Advanced glycation end products, oxidative stress and diabetic nephropathy. *Oxidative Medicine and Cellular Longevity*, 3(2), 101–108.
75. Zhang, X., Zhang, J.H., Chen, X.Y., Hu, Q.H., Wang, M.X., Jin, R., Zhang, Q. Y., Wang, W., Wang, R., Kang, L.L., Li, J.S., Li, M., Pan, Y., Huang, J.J. and Kong, L.D. (2015) Reactive oxygen species-induced TXNIP drives fructose-mediated hepatic inflammation and lipid accumulation through NLRP3 inflammasome activation. *Antioxidants and Redox Signaling*, 22(10), 848–870.
76. Zhang, Y.B., Meng, Y.H., Chang, S., Zhang, R.Y. and Shi, C. (2016) High fructose causes cardiac hypertrophy via mitochondrial signaling pathway. *American Journal of Translational Research*, 8(11), 4869–488

Appendices

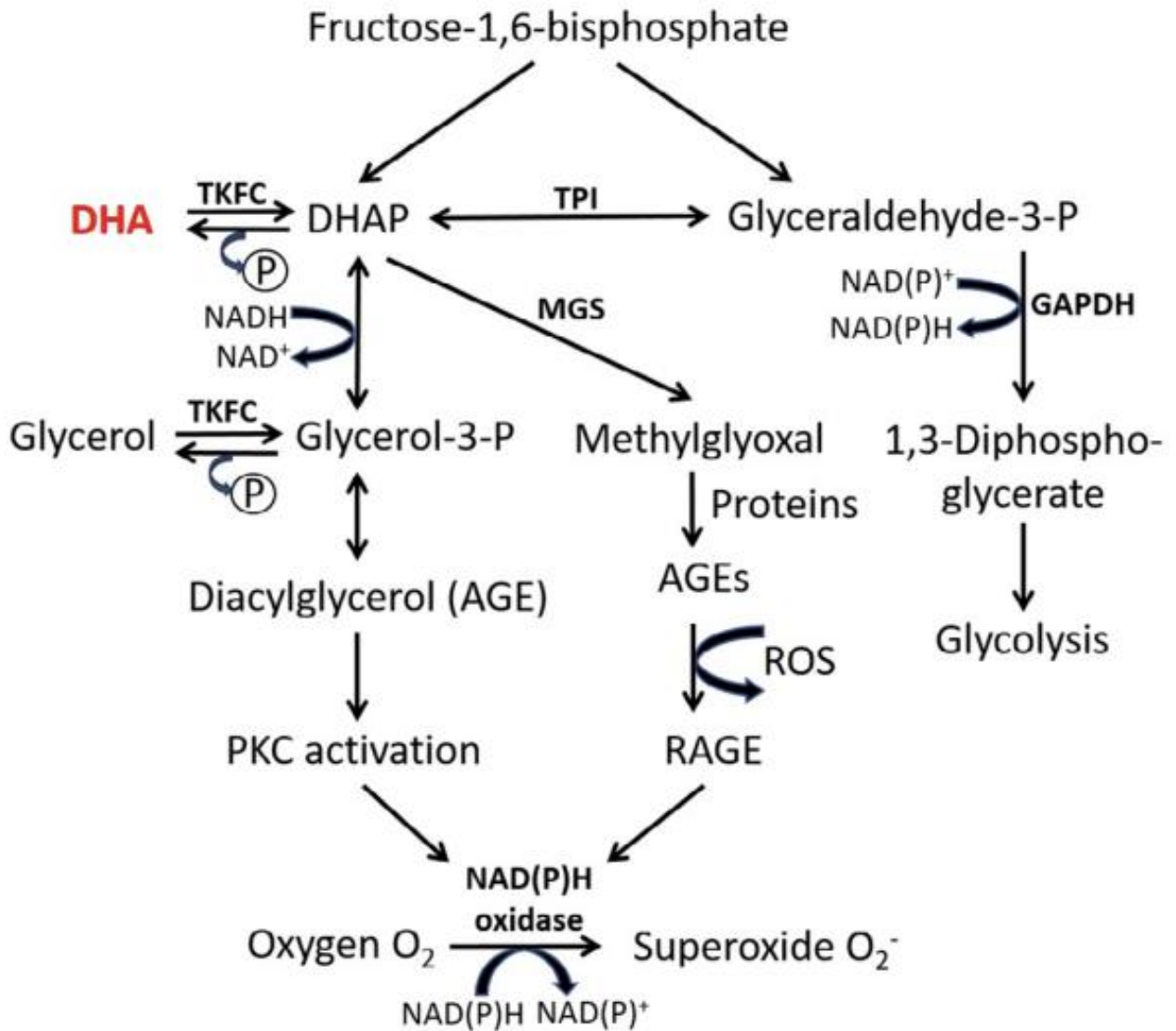


FIGURE 1. Fructose is converted into the two 3-carbon metabolites dihydroxyacetone phosphate (DHAP) and glyceraldehyde-3-phosphate (Glyceraldehyde-3-P). Exogenous dihydroxyacetone (DHA) is integrated into 3-carbon metabolism by phosphorylation to DHAP by triose kinase\FMN-cyclase (TKFC). DHAP and Glyceraldehyde-3-P are interconverted by triose phosphate isomerase (TPI). Glyceraldehyde-3-P is converted by Glyceraldehyde-3-

xliv

phosphate dehydrogenase (GAPDH) to 1,3-Diphospho-glycerate. DHAP can also be directly converted to methylglyoxal by methylglyoxal synthase (MGS). Methylglyoxal and Diacylglycerol are advanced glycation end products (AGE) which can interact with the receptor for advanced glycation end products (RAGE), activate protein kinase c (PKC), or even damage cellular proteins. AGEs and other reactive species like reactive oxygen species (ROS) can induce DNA, RNA, and protein damage which are detrimental to cell health and can induce cell death. Human nomenclature for enzymes is used for this summary figure.

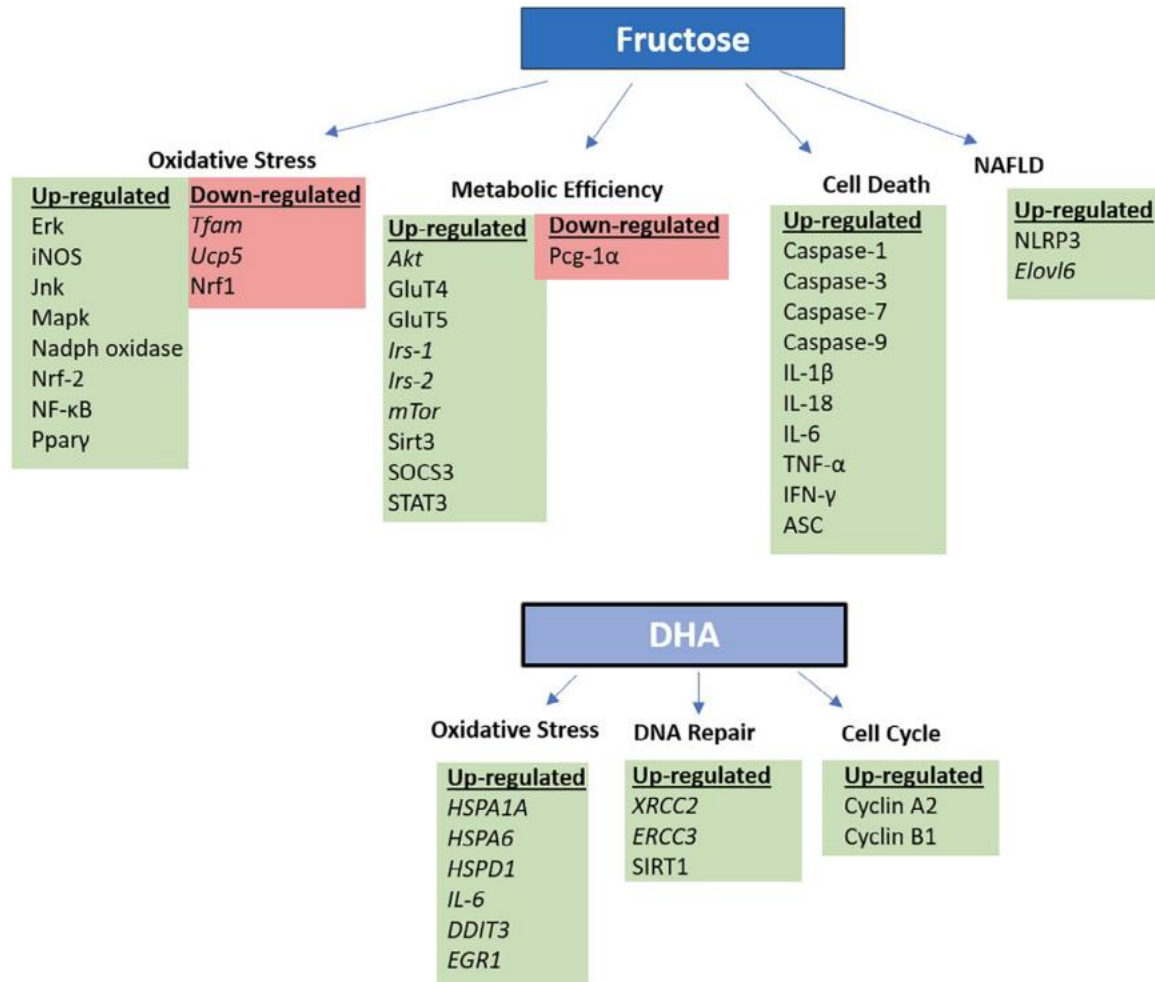


FIGURE 2. Both fructose and DHA exposures alter the expression of proteins involved in oxidative stress, metabolic efficiency, DNA repair, cell cycle control, and cell death. Changes in gene expression (italics) or protein levels identified in the summarized studies are presented here. Species is denoted by the use or lack of capitalization.

TABLE 1. Fructose exposures in cell line models.

Model-system	Dose	Exposure duration	Methods	Key findings	References
Reactive species formation					
Dendritic cells (human)	15 mM fructose	24–72 hr	ROS measured using flow cytometry to determine oxidation of dihydroethadamine 123 to rhodamine 123; AGE formation measured using AGE ELISA kits	Reduced level of ROS production in high fructose treated groups compared to high glucose and control groups	Jaiswal <i>et al.</i> , 2019
HEK293	30 mM fructose	4 hr	Total ROS production was quantified by DCFDA	ROS significantly increased in cells exposed to fructose and salt	Dornas <i>et al.</i> , 2017
HepG2	5 mM fructose	Incubation with 5 mM fructose for 48 hr and incubation with 2 μ M allopurinol or 20 μ M quercetin for additional 24 hr	Total ROS production was quantified by DCFDA	Elevated ROS, iNOS, and hydrogen peroxide levels in HepG2 cells	Zhang <i>et al.</i> , 2015
HLO2	5 mM fructose	Incubation with 5 mM fructose for 48 hr and incubation with 2 μ M allopurinol or 20 μ M quercetin for additional 24 hr	Total ROS production was quantified by DCFDA	Increases in ROS, iNOS, and hydrogen peroxide levels in HLO2 cells	Zhang <i>et al.</i> , 2015
Kupffer cells	5 mM fructose	Incubation with 5 mM fructose for 48 hr and incubation with 2 μ M allopurinol or 20 μ M quercetin for additional 24 hr	Total ROS production was quantified by DCFDA	No elevation in ROS, hydrogen peroxide, and MDA levels	Zhang <i>et al.</i> , 2015
L6 Myotubes	15 mM fructose	mtROS-1, 3, 6, and 24 hr; superoxide and hydrogen peroxide- 1, 3, and 6 hr	mtROS measured through MitoSOX red fluorescence; superoxide and hydrogen peroxide determined by fluorimetric assay	Increased production of mtROS with 1 hr and NO within 6 hr exposure; NO level reached maximum at 48 hr; non-mitochondrial respiration presented no significant change; iNOS levels peaked at 6 hr of exposure	Jaiswal <i>et al.</i> , 2015a
L6 Myotubes	15 mM fructose	1, 3, and 6 hr	Cytoplasmic ROS measured by DCFDA fluorescence	Time-dependent increase in ROS which peaked at 3 hr; oxidative stress results from increased content of ROS and/or RNS	Jaiswal <i>et al.</i> , 2015b
Rat hepatic parenchymal cell (RHPC)	5 mM fructose	Incubation with 5 mM fructose for 48 hr and incubation with 2 μ M allopurinol or 20 μ M quercetin for additional 24 hr	Total ROS production was quantified by DCFDA	Increased ROS, iNOS, and hydrogen peroxide levels	Zhang <i>et al.</i> , 2015
Mitochondrial and metabolic dysfunction					
Dendritic cells (human)	15 mM fructose	24–72 hr	Energetic state measurement- Seahorse analyzer	72 hr exposure induced shift from oxidative phosphorylation toward glycolysis compared to high glucose exposures; decrease in ECAR and OCR at 24 hr; fructose-treated cells exhibited the least OCR compared to all treatment and control groups	Jaiswal <i>et al.</i> , 2019

(Continues)

Model-system	Dose	Exposure duration	Methods	Key findings	References
Hepatocytes	5.5 mM fructose	72 hr	Apoptosis, lipid content, and lipid peroxidation measured through spectrometry, oxygen consumption monitored using Seahorse analyzer; liver steatosis and dysfunction measured through RT-qPCR	Elevated steatosis and liver dysfunction, increased apoptosis, oxidative stress and mitochondrial respiration	Grasselli et al., 2019
HepG2	5 mM fructose	5 mM fructose for 48 hr with 2 μ M allopurinol or 20 μ M quercetin for additional 24 hr	MMP detection	Altered mitochondrial membrane potential	Zhang et al., 2015
HLO2	5 mM fructose	5 mM fructose for 48 hr with 2 μ M allopurinol or 20 μ M quercetin for additional 24 hr	MMP detection	Altered mitochondrial membrane potential	Zhang et al., 2015
L6 Myotubes	15 mM fructose	mtDNA content and mitochondrial membrane potential- 3, 6, 24h, 48, and 72 hr; mitochondrial respiratory function- 3, 6, 24, and 48 hr	mtDNA content- PCR through amplification of a mitochondrial encoded gene; mitochondrial membrane potential- change analyzed with JC-1 absorption; mitochondrial respiratory function- Seahorse XF-e24 extracellular flux assay; ATP levels- stay Brite ATP assay; citrate synthase activity monitored by spectrophotometry	Reductions in mtDNA content; loss of mitochondrial membrane potential; impaired mitochondrial energy metabolism; decreased activities of citrate synthase, mitochondrial dehydrogenases, ATP-linked respiration, cellular ATP content, and mitochondrial respiratory complexes	Jaiswal et al., 2015a
L6 Myotubes	15 mM fructose	1, 3, and 6 hr	2-DG uptake assay	Reduction in 2-deoxyglucose uptake and an impairment of glucose utilization and insulin signaling through ROS-mediated activation of JNK and ERK1/2 pathways	Jaiswal et al., 2015b
RHPC	5 mM fructose	5 mM fructose for 48 hr with 2 μ M allopurinol or 20 μ M quercetin for additional 24 hr	MMP detection	Altered mitochondrial membrane potential	Zhang et al., 2015
Transcriptional changes					
3 T3-L1 Preadipocytes	550 μ M	48 hr	Protein expression measured by immunoblotting	Increase in adipogenesis and overexpression of Ppar γ , C/EBP α and Glut4	Du and Heaney, 2012

Model-system	Dose	Exposure duration	Methods	Key findings	References
3 T3-L1 Preadipocytes	30 mM fructose	Up to 8 days	mRNA expression measured using qPCR; protein expression measured by immunoblotting	FabP4, Ppar γ , C/Ebpa and 1 β -Hsd1 increased after 4, 6 and 8 days of exposure; C/Ebpa β decreased in same time period; GluT4 increased at days 4 through 6.	Legeza et al., 2014
Dendritic cells (human)	15 mM fructose	24–72 hr	CD86 expression measured through mean fluorescence intensity; NF- κ B activity determined through Alexa-594 antibody staining; IL-6 and IL-1 β determined with corresponding antibody	Increased expression of IL-6, IL-1 β , TNF- α , and CD86; exposure caused T-cells to increase secretion of IFN- γ ; increased production of AGEs led to activation of RAGE and expression of inflammatory cytokines; no significant difference in the expression of pAMPK- α , HIF-1 α and p70S6 kinase; GLUT-1 expression was 15% higher	Jaiswal et al., 2019
HEK293	30 mM fructose	4 hr	mRNA expression measured using qPCR; protein expression measured by immunoblotting	No significant change in SOD activity; NF- κ B subunit p65 was increased when exposed to fructose and salt together	Domas et al., 2017
Hepatocytes (primary rat)	5 mM fructose	5 mM fructose for 48 hr with 2 μ M allopurinol or 20 μ M quercetin for additional 24 hr	mRNA expression measured using qPCR; protein expression measured by immunoblotting	Increased protein expression levels of Txnip, Nlrp3, Asc, Caspase-1, Il-1 β and Il-18;	Zhang et al., 2015
HepG2	5 mM fructose	5 mM fructose for 48 hr with 2 μ M allopurinol or 20 μ M quercetin for additional 24 hr	mRNA expression measured using qPCR; protein expression measured by immunoblotting	Increased expression of TXNIP and NLRP3 levels; 72 hr exposure led to increased levels of ASC, Caspase-1, STAT3, SOCS3, IL-18, and IL-1 β	Zhang et al., 2015
HLO2	5 mM fructose	5 mM fructose for 48 hr with 2 μ M allopurinol or 20 μ M quercetin for additional 24 hr	mRNA expression measured using qPCR; protein expression measured by immunoblotting	Increased expression of TXNIP and NLRP3 levels; 72 hr exposure led to increased levels of ASC, Caspase-1, STAT3, SOCS3, IL-18, and IL-1 β	Zhang et al., 2015
L6 Myotubes	15 mM fructose	inos expression- 3, 6, 24, 48, and 72 hr; Nrf-2 translocation- 24 and 48 hr	Nitrite values determined with differing concentrations of sodium nitrite as a standard; Nrf-2 expression monitored by immunofluorescence; cytochrome C levels determined by immunoblotting	Increased NO production and iNOS expression; iNOS expression highest at 6 hr; elevated localization of Nrf-2 to the nucleus at 24 and 48 hr; apoptosis evident by increased levels of cleaved caspase 3, 9 and 7; Bcl-2 protein expression was significantly reduced and there was an increase in Bax; 48 and 72 hr exposure elevated cytochrome C levels in the cytoplasm from the mitochondria	Jaiswal et al., 2015a

(Continues)

Model-system	Dose	Exposure duration	Methods	Key findings	References
L6 Myotubes	15 mM fructose	1, 3, and 6 hr	GluT4 translocation measured by the cell surface level of GluT4myc through an antibody-based colorimetric assay; mRNA expression measured using qPCR; protein expression measured by immunoblotting	GluT1 and GluT4 protein and mRNA levels not altered at 3 and 6 hr; no significant change in <i>GluT5</i> mRNA expression; impaired insulin-stimulated translocation of GluT4myc to the cell surface; lower insulin-stimulated tyrosine phosphorylation of <i>Irs-1</i> ; no differences in <i>Irs-1</i> protein expression; inhibition of insulin-stimulated phosphorylation of Akt without altered total amount of Akt; no altered mRNA expression of <i>Irs-1</i> , <i>PI3k</i> , <i>Akt</i> , <i>GluT4</i> , and <i>GluT1</i> ; elevated ROS activated Jnk, Erk, p38, MapK, and Nf- κ b inflammation pathways; increased phosphorylation of Jnk and Erk1/2 without any significant change in the total content; increase in the activity of Nf- κ b pathway	Jaiswal <i>et al.</i> , 2015b
Rat hepatic parenchymal cell (RHPC)	5 mM fructose	5 mM fructose for 48 hr with 2 μ M allopurinol or 20 μ M quercetin for additional 24 hr	mRNA expression measured using qPCR; protein expression measured by immunoblotting	Increased expression of <i>Txnip</i> and <i>Nlrp3</i> levels; 72 hr exposure led to increased levels of <i>Asc</i> , <i>Caspase-1</i> , <i>Stat3</i> , <i>Socs3</i> , <i>Il-18</i> , and <i>Il-1β</i>	Zhang <i>et al.</i> , 2015

TABLE 2. Fructose exposures in animal models.

Model-system	Dose	Exposure duration	Methods	Key findings	References
Reactive species formation					
Male Wistar rats	High-fat diet and 5% fructose in drinking water per day	4 months	ROS in kidney measured DCFDA; MDA measured spectrophotometrically	ROS and malondialdehyde expression were elevated in the kidneys	Rosas-Villegas <i>et al.</i> , 2017
Male C57BL/6 mice	10% fructose in drinking water per day	20 weeks	Total ROS activity assay kit	80% increase in ROS production; increased mitochondrial hydrogen peroxide production	Zhang <i>et al.</i> , 2016
Male Sprague-Dawley rats	10% fructose in drinking water per day	8 weeks	Total ROS measured by DCFDA	Increased ROS, MDA, XO, iNOS, and hydrogen peroxide levels in rat livers	Zhang <i>et al.</i> , 2015
Male HTG rats, male Wistar rats, and male Lewis rats	10% fructose in drinking water per day	3 weeks	Pentidine measurement- fluorescence at 332ex/378em nm	Increased post-translational pentosidine levels in rat aorta and skin samples for all three strains of rats	Mikulikova <i>et al.</i> , 2008
Male Wistar rats (mononuclear cells)	10% fructose in drinking water per day	12 weeks	ROS measured using flow cytometry to quantify the production of *O_2 , H_2O_2 , NO and $^*ONOO^-/^*OH^-$, with DHE, DCF, DAF-2 T in peripheral blood and bone-marrow mononuclear cells	Elevated level of ROS generation in peripheral blood mononuclear cells; no ROS increase in bone marrow mononuclear cells	Porto <i>et al.</i> , 2015
Male Fischer rats	20% fructose in drinking water per day and high salt diet (8%) for last 10 weeks	20 weeks	ROS production quantified using DCFDA; SOD activity measured by autooxidation of pyrogallol; cat activity was measured spectrophotometrically	Salt-dependent hypertension and elevated oxidative stress; decrease in renal enzymatic SOD and catalase activity in the kidney	Domas <i>et al.</i> , 2017
Male and female Sprague-Dawley rats	20% fructose water solution per day	Dose received during gestation and lactation periods	OxiSelect in vitro ROS/RNS assay kit	1.5-fold increase in hippocampal LPO which is associated with elevated ROS	Yamada <i>et al.</i> , 2019
Male Wistar rats	250 mL of 25% fructose drinking water per day with 40.6% fats	6 weeks	ROS levels measured by DCFDA	8-time increase in lipid peroxidation levels in mitochondria for fructose groups and high fat and fructose groups; no increases in ROS for fructose-treated groups	Garcia-Berumen <i>et al.</i> , 2019
Male Sprague-Dawley rats	30 g of fructose per 100 g of 8 weeks chow (30% fructose)	8 weeks	DNA/RNA oxidative damage ELISA assay	8-OHdG levels were increased indicating elevated levels of oxidative stress	Cioffi <i>et al.</i> , 2017
Male C57BL/6 mice	60% fructose diet per day	6, 10, and 20 weeks	Superoxide production determined through measurement of NADPH activity	Significant increase in superoxide production in mice during 6 weeks of intake; at 10 weeks, there was a 29% increase in superoxide production, and at 20 weeks, there was a 16% increase	Mellor <i>et al.</i> , 2010
Male Wistar rats	Fructose content provides 60% of calories in diet per day	2 weeks	Measured through insulin resistance	Inhibited expression of catalase in the heart and liver; condition leads to a high vulnerability to elevated levels of oxidative stress in insulin resistance	Cavarape <i>et al.</i> , 2001

(Continues)

Model-system	Dose	Exposure duration	Methods	Key findings	References
Male spontaneously hypertensive rats	60% fructose	3 weeks	ROS by flow cytometry using the fluorescence dye DHE	There were high levels of ROS accumulation and lipid peroxidation in rostral ventrolateral medulla; development of brain oxidative stress can lead to hypertension	Wu et al., 2017
Male Wistar rats	60% fructose chow in diet per day	12, 16, 20, and 24 weeks	MDA measured spectrophotometrically	Increase in production of substances such as methylglyoxal, which leads to muscle oxidative stress; no significant increase in the levels of the peroxidation product malondialdehyde in the serum, left ventricular tissue, or in the cardiac level of the nitrooxidative marker 3-nitrotyrosine	Szucs et al., 2019
Mitochondrial and metabolic dysfunction					
Male C57BL/6 mice	10% fructose in drinking water per day	20 weeks	Oxygen consumption rates monitored by a Seahorse XF24 oxygen flux analyzer; complex II enzyme activity measured using microplate assay kit	Cardiac hypertrophy, diastolic dysfunction, decreased complex II activity by 60%, and reduced state III and IV OCR; for complex I and II, rates of ATP synthesis decreased by 37% and 36% respectively	Zhang et al., 2016
Male Sprague-Dawley rats	10% fructose in drinking water per day	6 weeks	Respiratory measurements made using Oroboros system for permeabilized muscle fibers	In the extensor digitorum longus (EDL) muscle, there was a significant decrease in complex I respiration; respiratory activity for other complexes were similar; for the soleus muscle, OXPHOS capacity for complex II was much lower	Warren et al., 2014
Male Wistar rats	250 mL of 25% fructose drinking water per day	6 weeks	Mitochondrial respiration obtained by determining the oxygen consumption rate of isolated mitochondria using a Clark-type electrode coupled to a YSI 5300A biological oxygen monitor	Mitochondrial respiratory rate in state 3 decreased in the fructose group by 1.6-fold; 1.8-fold increase in state 4 respiration; complex I activity decreased ~2.3-fold in mitochondria for the high fructose group	Garcia-Berumen et al., 2019
Male Sprague-Dawley rats	30 g of fructose per 100 g of 8 weeks chow (30% fructose)	8 weeks	mtDNA damage measured using qPCR; changes in mitochondrial biogenesis monitored through the expression of Pcg1 α , Nrf1, and Tfam	Increase in mtDNA damage in the liver of rats; 22% decrease in mtDNA fragments; mitochondrial copy number was reduced by approximately 56%; reduced mitochondrial biogenesis	Cioffi et al., 2017
Male and female Sprague-Dawley rats	20% fructose water solution per day	Dose received during gestation and lactation periods	Mitochondria oxygen consumption rate-MitoXpress oxygen consumption assay; mtDNA damage assessed using qPCR	Reduction mitochondrial OCR; no change in mtDNA amount	Yamada et al., 2019

Model-system	Dose	Exposure duration	Methods	Key findings	References
Transcriptional changes					
Male Wistar rats	High-fat diet and 5% fructose in drinking water per day	4 months	Protein expression measured by immunoblotting	Increased protein expression of inflammatory markers Tlr-4, Nf- κ b; Tnf α / β , and Mcp1	Rosas-Villegas et al., 2017
Kupffer cells from male Sprague-Dawley rats	10% fructose in drinking water per day	8 weeks	mRNA expression measured using qPCR	Increase in Txnip, Nlrp3 levels in Kupffer cells, and aggravate oxidative stress in livers; in vitro fructose exposure did not change levels of Txnip, Nlrp3, and no ROS overproduction; increased co-localization of Nlrp3;	Zhang et al., 2015
Male Sprague-Dawley rats	30 g of fructose per 100 g of chow (30% fructose)	8 weeks	mRNA expression measured using qPCR; protein expression measured by immunoblotting	Pgc1 α , Nrf1, and Tfam reduced expression by 19%, 41%, and 43% respectively	Cioffi et al., 2017
Male C57BL/6 mice	10% fructose in drinking water per day	20 weeks	mRNA expression measured using qPCR; protein expression measured by immunoblotting	Decreased CFTR expression and induced ROS and oxidative stress	Zhang et al., 2016
Male Sprague-Dawley rats	10% fructose in drinking water per day	6 weeks	Protein expression measured by immunoblotting	Decline in Pgc-1 α protein levels in both EDL and soleus muscles; increased Sirt3 protein levels in the soleus, and decline in the EDL; no changes in thioredoxin reductase-2 protein levels in the soleus, but there was a decrease in the EDL muscle	Warren et al., 2014
Male Wistar rats	10% fructose in drinking water per day	12 weeks	Annexin V-FITC apoptosis detection kit; cytokines measured in the plasma by flow cytometry using a Cytometric bead Array - Mouse inflammation kit	Elevated rates of apoptosis; Il-6 and Il-12p70 were higher	Porto et al., 2015
Male and female Wistar rats	10% fructose in drinking water per day	24 weeks	mRNA expression measured using qPCR	Increased expression of <i>Irf1</i> , <i>Irf3</i> , <i>Irf7</i> , <i>Irf8</i> , <i>Irf9</i> , <i>Irf10</i> , <i>Irf11</i> , <i>Irf12</i> , <i>Irf13</i> , <i>Irf14</i> , <i>Irf15</i> , <i>Irf16</i> , <i>Irf17</i> , <i>Irf18</i> , <i>Irf19</i> , <i>Irf20</i> , <i>Irf21</i> , <i>Irf22</i> , <i>Irf23</i> , <i>Irf24</i> , <i>Irf25</i> , <i>Irf26</i> , <i>Irf27</i> , <i>Irf28</i> , <i>Irf29</i> , <i>Irf30</i> , <i>Irf31</i> , <i>Irf32</i> , <i>Irf33</i> , <i>Irf34</i> , <i>Irf35</i> , <i>Irf36</i> , <i>Irf37</i> , <i>Irf38</i> , <i>Irf39</i> , <i>Irf40</i> , <i>Irf41</i> , <i>Irf42</i> , <i>Irf43</i> , <i>Irf44</i> , <i>Irf45</i> , <i>Irf46</i> , <i>Irf47</i> , <i>Irf48</i> , <i>Irf49</i> , <i>Irf50</i> , <i>Irf51</i> , <i>Irf52</i> , <i>Irf53</i> , <i>Irf54</i> , <i>Irf55</i> , <i>Irf56</i> , <i>Irf57</i> , <i>Irf58</i> , <i>Irf59</i> , <i>Irf60</i> , <i>Irf61</i> , <i>Irf62</i> , <i>Irf63</i> , <i>Irf64</i> , <i>Irf65</i> , <i>Irf66</i> , <i>Irf67</i> , <i>Irf68</i> , <i>Irf69</i> , <i>Irf70</i> , <i>Irf71</i> , <i>Irf72</i> , <i>Irf73</i> , <i>Irf74</i> , <i>Irf75</i> , <i>Irf76</i> , <i>Irf77</i> , <i>Irf78</i> , <i>Irf79</i> , <i>Irf80</i> , <i>Irf81</i> , <i>Irf82</i> , <i>Irf83</i> , <i>Irf84</i> , <i>Irf85</i> , <i>Irf86</i> , <i>Irf87</i> , <i>Irf88</i> , <i>Irf89</i> , <i>Irf90</i> , <i>Irf91</i> , <i>Irf92</i> , <i>Irf93</i> , <i>Irf94</i> , <i>Irf95</i> , <i>Irf96</i> , <i>Irf97</i> , <i>Irf98</i> , <i>Irf99</i> , <i>Irf100</i> , <i>Irf101</i> , <i>Irf102</i> , <i>Irf103</i> , <i>Irf104</i> , <i>Irf105</i> , <i>Irf106</i> , <i>Irf107</i> , <i>Irf108</i> , <i>Irf109</i> , <i>Irf110</i> , <i>Irf111</i> , <i>Irf112</i> , <i>Irf113</i> , <i>Irf114</i> , <i>Irf115</i> , <i>Irf116</i> , <i>Irf117</i> , <i>Irf118</i> , <i>Irf119</i> , <i>Irf120</i> , <i>Irf121</i> , <i>Irf122</i> , <i>Irf123</i> , <i>Irf124</i> , <i>Irf125</i> , <i>Irf126</i> , <i>Irf127</i> , <i>Irf128</i> , <i>Irf129</i> , <i>Irf130</i> , <i>Irf131</i> , <i>Irf132</i> , <i>Irf133</i> , <i>Irf134</i> , <i>Irf135</i> , <i>Irf136</i> , <i>Irf137</i> , <i>Irf138</i> , <i>Irf139</i> , <i>Irf140</i> , <i>Irf141</i> , <i>Irf142</i> , <i>Irf143</i> , <i>Irf144</i> , <i>Irf145</i> , <i>Irf146</i> , <i>Irf147</i> , <i>Irf148</i> , <i>Irf149</i> , <i>Irf150</i> , <i>Irf151</i> , <i>Irf152</i> , <i>Irf153</i> , <i>Irf154</i> , <i>Irf155</i> , <i>Irf156</i> , <i>Irf157</i> , <i>Irf158</i> , <i>Irf159</i> , <i>Irf160</i> , <i>Irf161</i> , <i>Irf162</i> , <i>Irf163</i> , <i>Irf164</i> , <i>Irf165</i> , <i>Irf166</i> , <i>Irf167</i> , <i>Irf168</i> , <i>Irf169</i> , <i>Irf170</i> , <i>Irf171</i> , <i>Irf172</i> , <i>Irf173</i> , <i>Irf174</i> , <i>Irf175</i> , <i>Irf176</i> , <i>Irf177</i> , <i>Irf178</i> , <i>Irf179</i> , <i>Irf180</i> , <i>Irf181</i> , <i>Irf182</i> , <i>Irf183</i> , <i>Irf184</i> , <i>Irf185</i> , <i>Irf186</i> , <i>Irf187</i> , <i>Irf188</i> , <i>Irf189</i> , <i>Irf190</i> , <i>Irf191</i> , <i>Irf192</i> , <i>Irf193</i> , <i>Irf194</i> , <i>Irf195</i> , <i>Irf196</i> , <i>Irf197</i> , <i>Irf198</i> , <i>Irf199</i> , <i>Irf200</i> , <i>Irf201</i> , <i>Irf202</i> , <i>Irf203</i> , <i>Irf204</i> , <i>Irf205</i> , <i>Irf206</i> , <i>Irf207</i> , <i>Irf208</i> , <i>Irf209</i> , <i>Irf210</i> , <i>Irf211</i> , <i>Irf212</i> , <i>Irf213</i> , <i>Irf214</i> , <i>Irf215</i> , <i>Irf216</i> , <i>Irf217</i> , <i>Irf218</i> , <i>Irf219</i> , <i>Irf220</i> , <i>Irf221</i> , <i>Irf222</i> , <i>Irf223</i> , <i>Irf224</i> , <i>Irf225</i> , <i>Irf226</i> , <i>Irf227</i> , <i>Irf228</i> , <i>Irf229</i> , <i>Irf230</i> , <i>Irf231</i> , <i>Irf232</i> , <i>Irf233</i> , <i>Irf234</i> , <i>Irf235</i> , <i>Irf236</i> , <i>Irf237</i> , <i>Irf238</i> , <i>Irf239</i> , <i>Irf240</i> , <i>Irf241</i> , <i>Irf242</i> , <i>Irf243</i> , <i>Irf244</i> , <i>Irf245</i> , <i>Irf246</i> , <i>Irf247</i> , <i>Irf248</i> , <i>Irf249</i> , <i>Irf250</i> , <i>Irf251</i> , <i>Irf252</i> , <i>Irf253</i> , <i>Irf254</i> , <i>Irf255</i> , <i>Irf256</i> , <i>Irf257</i> , <i>Irf258</i> , <i>Irf259</i> , <i>Irf260</i> , <i>Irf261</i> , <i>Irf262</i> , <i>Irf263</i> , <i>Irf264</i> , <i>Irf265</i> , <i>Irf266</i> , <i>Irf267</i> , <i>Irf268</i> , <i>Irf269</i> , <i>Irf270</i> , <i>Irf271</i> , <i>Irf272</i> , <i>Irf273</i> , <i>Irf274</i> , <i>Irf275</i> , <i>Irf276</i> , <i>Irf277</i> , <i>Irf278</i> , <i>Irf279</i> , <i>Irf280</i> , <i>Irf281</i> , <i>Irf282</i> , <i>Irf283</i> , <i>Irf284</i> , <i>Irf285</i> , <i>Irf286</i> , <i>Irf287</i> , <i>Irf288</i> , <i>Irf289</i> , <i>Irf290</i> , <i>Irf291</i> , <i>Irf292</i> , <i>Irf293</i> , <i>Irf294</i> , <i>Irf295</i> , <i>Irf296</i> , <i>Irf297</i> , <i>Irf298</i> , <i>Irf299</i> , <i>Irf300</i> , <i>Irf301</i> , <i>Irf302</i> , <i>Irf303</i> , <i>Irf304</i> , <i>Irf305</i> , <i>Irf306</i> , <i>Irf307</i> , <i>Irf308</i> , <i>Irf309</i> , <i>Irf310</i> , <i>Irf311</i> , <i>Irf312</i> , <i>Irf313</i> , <i>Irf314</i> , <i>Irf315</i> , <i>Irf316</i> , <i>Irf317</i> , <i>Irf318</i> , <i>Irf319</i> , <i>Irf320</i> , <i>Irf321</i> , <i>Irf322</i> , <i>Irf323</i> , <i>Irf324</i> , <i>Irf325</i> , <i>Irf326</i> , <i>Irf327</i> , <i>Irf328</i> , <i>Irf329</i> , <i>Irf330</i> , <i>Irf331</i> , <i>Irf332</i> , <i>Irf333</i> , <i>Irf334</i> , <i>Irf335</i> , <i>Irf336</i> , <i>Irf337</i> , <i>Irf338</i> , <i>Irf339</i> , <i>Irf340</i> , <i>Irf341</i> , <i>Irf342</i> , <i>Irf343</i> , <i>Irf344</i> , <i>Irf345</i> , <i>Irf346</i> , <i>Irf347</i> , <i>Irf348</i> , <i>Irf349</i> , <i>Irf350</i> , <i>Irf351</i> , <i>Irf352</i> , <i>Irf353</i> , <i>Irf354</i> , <i>Irf355</i> , <i>Irf356</i> , <i>Irf357</i> , <i>Irf358</i> , <i>Irf359</i> , <i>Irf360</i> , <i>Irf361</i> , <i>Irf362</i> , <i>Irf363</i> , <i>Irf364</i> , <i>Irf365</i> , <i>Irf366</i> , <i>Irf367</i> , <i>Irf368</i> , <i>Irf369</i> , <i>Irf370</i> , <i>Irf371</i> , <i>Irf372</i> , <i>Irf373</i> , <i>Irf374</i> , <i>Irf375</i> , <i>Irf376</i> , <i>Irf377</i> , <i>Irf378</i> , <i>Irf379</i> , <i>Irf380</i> , <i>Irf381</i> , <i>Irf382</i> , <i>Irf383</i> , <i>Irf384</i> , <i>Irf385</i> , <i>Irf386</i> , <i>Irf387</i> , <i>Irf388</i> , <i>Irf389</i> , <i>Irf390</i> , <i>Irf391</i> , <i>Irf392</i> , <i>Irf393</i> , <i>Irf394</i> , <i>Irf395</i> , <i>Irf396</i> , <i>Irf397</i> , <i>Irf398</i> , <i>Irf399</i> , <i>Irf400</i> , <i>Irf401</i> , <i>Irf402</i> , <i>Irf403</i> , <i>Irf404</i> , <i>Irf405</i> , <i>Irf406</i> , <i>Irf407</i> , <i>Irf408</i> , <i>Irf409</i> , <i>Irf410</i> , <i>Irf411</i> , <i>Irf412</i> , <i>Irf413</i> , <i>Irf414</i> , <i>Irf415</i> , <i>Irf416</i> , <i>Irf417</i> , <i>Irf418</i> , <i>Irf419</i> , <i>Irf420</i> , <i>Irf421</i> , <i>Irf422</i> , <i>Irf423</i> , <i>Irf424</i> , <i>Irf425</i> , <i>Irf426</i> , <i>Irf427</i> , <i>Irf428</i> , <i>Irf429</i> , <i>Irf430</i> , <i>Irf431</i> , <i>Irf432</i> , <i>Irf433</i> , <i>Irf434</i> , <i>Irf435</i> , <i>Irf436</i> , <i>Irf437</i> , <i>Irf438</i> , <i>Irf439</i> , <i>Irf440</i> , <i>Irf441</i> , <i>Irf442</i> , <i>Irf443</i> , <i>Irf444</i> , <i>Irf445</i> , <i>Irf446</i> , <i>Irf447</i> , <i>Irf448</i> , <i>Irf449</i> , <i>Irf450</i> , <i>Irf451</i> , <i>Irf452</i> , <i>Irf453</i> , <i>Irf454</i> , <i>Irf455</i> , <i>Irf456</i> , <i>Irf457</i> , <i>Irf458</i> , <i>Irf459</i> , <i>Irf460</i> , <i>Irf461</i> , <i>Irf462</i> , <i>Irf463</i> , <i>Irf464</i> , <i>Irf465</i> , <i>Irf466</i> , <i>Irf467</i> , <i>Irf468</i> , <i>Irf469</i> , <i>Irf470</i> , <i>Irf471</i> , <i>Irf472</i> , <i>Irf473</i> , <i>Irf474</i> , <i>Irf475</i> , <i>Irf476</i> , <i>Irf477</i> , <i>Irf478</i> , <i>Irf479</i> , <i>Irf480</i> , <i>Irf481</i> , <i>Irf482</i> , <i>Irf483</i> , <i>Irf484</i> , <i>Irf485</i> , <i>Irf486</i> , <i>Irf487</i> , <i>Irf488</i> , <i>Irf489</i> , <i>Irf490</i> , <i>Irf491</i> , <i>Irf492</i> , <i>Irf493</i> , <i>Irf494</i> , <i>Irf495</i> , <i>Irf496</i> , <i>Irf497</i> , <i>Irf498</i> , <i>Irf499</i> , <i>Irf500</i> , <i>Irf501</i> , <i>Irf502</i> , <i>Irf503</i> , <i>Irf504</i> , <i>Irf505</i> , <i>Irf506</i> , <i>Irf507</i> , <i>Irf508</i> , <i>Irf509</i> , <i>Irf510</i> , <i>Irf511</i> , <i>Irf512</i> , <i>Irf513</i> , <i>Irf514</i> , <i>Irf515</i> , <i>Irf516</i> , <i>Irf517</i> , <i>Irf518</i> , <i>Irf519</i> , <i>Irf520</i> , <i>Irf521</i> , <i>Irf522</i> , <i>Irf523</i> , <i>Irf524</i> , <i>Irf525</i> , <i>Irf526</i> , <i>Irf527</i> , <i>Irf528</i> , <i>Irf529</i> , <i>Irf530</i> , <i>Irf531</i> , <i>Irf532</i> , <i>Irf533</i> , <i>Irf534</i> , <i>Irf535</i> , <i>Irf536</i> , <i>Irf537</i> , <i>Irf538</i> , <i>Irf539</i> , <i>Irf540</i> , <i>Irf541</i> , <i>Irf542</i> , <i>Irf543</i> , <i>Irf544</i> , <i>Irf545</i> , <i>Irf546</i> , <i>Irf547</i> , <i>Irf548</i> , <i>Irf549</i> , <i>Irf550</i> , <i>Irf551</i> , <i>Irf552</i> , <i>Irf553</i> , <i>Irf554</i> , <i>Irf555</i> , <i>Irf556</i> , <i>Irf557</i> , <i>Irf558</i> , <i>Irf559</i> , <i>Irf560</i> , <i>Irf561</i> , <i>Irf562</i> , <i>Irf563</i> , <i>Irf564</i> , <i>Irf565</i> , <i>Irf566</i> , <i>Irf567</i> , <i>Irf568</i> , <i>Irf569</i> , <i>Irf570</i> , <i>Irf571</i> , <i>Irf572</i> , <i>Irf573</i> , <i>Irf574</i> , <i>Irf575</i> , <i>Irf576</i> , <i>Irf577</i> , <i>Irf578</i> , <i>Irf579</i> , <i>Irf580</i> , <i>Irf581</i> , <i>Irf582</i> , <i>Irf583</i> , <i>Irf584</i> , <i>Irf585</i> , <i>Irf586</i> , <i>Irf587</i> , <i>Irf588</i> , <i>Irf589</i> , <i>Irf590</i> , <i>Irf591</i> , <i>Irf592</i> , <i>Irf593</i> , <i>Irf594</i> , <i>Irf595</i> , <i>Irf596</i> , <i>Irf597</i> , <i>Irf598</i> , <i>Irf599</i> , <i>Irf600</i> , <i>Irf601</i> , <i>Irf602</i> , <i>Irf603</i> , <i>Irf604</i> , <i>Irf605</i> , <i>Irf606</i> , <i>Irf607</i> , <i>Irf608</i> , <i>Irf609</i> , <i>Irf610</i> , <i>Irf611</i> , <i>Irf612</i> , <i>Irf613</i> , <i>Irf614</i> , <i>Irf615</i> , <i>Irf616</i> , <i>Irf617</i> , <i>Irf618</i> , <i>Irf619</i> , <i>Irf620</i> , <i>Irf621</i> , <i>Irf622</i> , <i>Irf623</i> , <i>Irf624</i> , <i>Irf625</i> , <i>Irf626</i> , <i>Irf627</i> , <i>Irf628</i> , <i>Irf629</i> , <i>Irf630</i> , <i>Irf631</i> , <i>Irf632</i> , <i>Irf633</i> , <i>Irf634</i> , <i>Irf635</i> , <i>Irf636</i> , <i>Irf637</i> , <i>Irf638</i> , <i>Irf639</i> , <i>Irf640</i> , <i>Irf641</i> , <i>Irf642</i> , <i>Irf643</i> , <i>Irf644</i> , <i>Irf645</i> , <i>Irf646</i> , <i>Irf647</i> , <i>Irf648</i> , <i>Irf649</i> , <i>Irf650</i> , <i>Irf651</i> , <i>Irf652</i> , <i>Irf653</i> , <i>Irf654</i> , <i>Irf655</i> , <i>Irf656</i> , <i>Irf657</i> , <i>Irf658</i> , <i>Irf659</i> , <i>Irf660</i> , <i>Irf661</i> , <i>Irf662</i> , <i>Irf663</i> , <i>Irf664</i> , <i>Irf665</i> , <i>Irf666</i> , <i>Irf667</i> , <i>Irf668</i> , <i>Irf669</i> , <i>Irf670</i> , <i>Irf671</i> , <i>Irf672</i> , <i>Irf673</i> , <i>Irf674</i> , <i>Irf675</i> , <i>Irf676</i> , <i>Irf677</i> , <i>Irf678</i> , <i>Irf679</i> , <i>Irf680</i> , <i>Irf681</i> , <i>Irf682</i> , <i>Irf683</i> , <i>Irf684</i> , <i>Irf685</i> , <i>Irf686</i> , <i>Irf687</i> , <i>Irf688</i> , <i>Irf689</i> , <i>Irf690</i> , <i>Irf691</i> , <i>Irf692</i> , <i>Irf693</i> , <i>Irf694</i> , <i>Irf695</i> , <i>Irf696</i> , <i>Irf697</i> , <i>Irf698</i> , <i>Irf699</i> , <i>Irf700</i> , <i>Irf701</i> , <i>Irf702</i> , <i>Irf703</i> , <i>Irf704</i> , <i>Irf705</i> , <i>Irf706</i> , <i>Irf707</i> , <i>Irf708</i> , <i>Irf709</i> , <i>Irf710</i> , <i>Irf711</i> , <i>Irf712</i> , <i>Irf713</i> , <i>Irf714</i> , <i>Irf715</i> , <i>Irf716</i> , <i>Irf717</i> , <i>Irf718</i> , <i>Irf719</i> , <i>Irf720</i> , <i>Irf721</i> , <i>Irf722</i> , <i>Irf723</i> , <i>Irf724</i> , <i>Irf725</i> , <i>Irf726</i> , <i>Irf727</i> , <i>Irf728</i> , <i>Irf729</i> , <i>Irf730</i> , <i>Irf731</i> , <i>Irf732</i> , <i>Irf733</i> , <i>Irf734</i> , <i>Irf735</i> , <i>Irf736</i> , <i>Irf737</i> , <i>Irf738</i> , <i>Irf739</i> , <i>Irf740</i> , <i>Irf741</i> , <i>Irf742</i> , <i>Irf743</i> , <i>Irf744</i> , <i>Irf745</i> , <i>Irf746</i> , <i>Irf747</i> , <i>Irf748</i> , <i>Irf749</i> , <i>Irf750</i> , <i>Irf751</i> , <i>Irf752</i> , <i>Irf753</i> , <i>Irf754</i> , <i>Irf755</i> , <i>Irf756</i> , <i>Irf757</i> , <i>Irf758</i> , <i>Irf759</i> , <i>Irf760</i> , <i>Irf761</i> , <i>Irf762</i> , <i>Irf763</i> , <i>Irf764</i> , <i>Irf765</i> , <i>Irf766</i> , <i>Irf767</i> , <i>Irf768</i> , <i>Irf769</i> , <i>Irf770</i> , <i>Irf771</i> , <i>Irf772</i> , <i>Irf773</i> , <i>Irf774</i> , <i>Irf775</i> , <i>Irf776</i> , <i>Irf777</i> , <i>Irf778</i> , <i>Irf779</i> , <i>Irf780</i> , <i>Irf781</i> , <i>Irf782</i> , <i>Irf783</i> , <i>Irf784</i> , <i>Irf785</i> , <i>Irf786</i> , <i>Irf787</i> , <i>Irf788</i> , <i>Irf789</i> , <i>Irf790</i> , <i>Irf791</i> , <i>Irf792</i> , <i>Irf793</i> , <i>Irf794</i> , <i>Irf795</i> , <i>Irf796</i> , <i>Irf797</i> , <i>Irf798</i> , <i>Irf799</i> , <i>Irf800</i> , <i>Irf801</i> , <i>Irf802</i> , <i>Irf803</i> , <i>Irf804</i> , <i>Irf805</i> , <i>Irf806</i> , <i>Irf807</i> , <i>Irf808</i> , <i>Irf809</i> , <i>Irf810</i> , <i>Irf811</i> , <i>Irf812</i> , <i>Irf813</i> , <i>Irf814</i> , <i>Irf815</i> , <i>Irf816</i> , <i>Irf817</i> , <i>Irf818</i> , <i>Irf819</i> , <i>Irf820</i> , <i>Irf821</i> , <i>Irf822</i> , <i>Irf823</i> , <i>Irf824</i> , <i>Irf825</i> , <i>Irf826</i> , <i>Irf827</i> , <i>Irf828</i> , <i>Irf829</i> , <i>Irf830</i> , <i>Irf831</i> , <i>Irf832</i> , <i>Irf833</i> , <i>Irf834</i> , <i>Irf835</i> , <i>Irf836</i> , <i>Irf837</i> , <i>Irf838</i> , <i>Irf839</i> , <i>Irf840</i> , <i>Irf841</i> , <i>Irf842</i> , <i>Irf843</i> , <i>Irf844</i> , <i>Irf845</i> , <i>Irf846</i> , <i>Irf847</i> , <i>Irf848</i> , <i>Irf849</i> , <i>Irf850</i> , <i>Irf851</i> , <i>Irf852</i> , <i>Irf853</i> , <i>Irf854</i> , <i>Irf855</i> , <i>Irf856</i> , <i>Irf857</i> , <i>Irf858</i> , <i>Irf859</i> , <i>Irf860</i> , <i>Irf861</i> , <i>Irf862</i> , <i>Irf863</i> , <i>Irf864</i> , <i>Irf865</i> , <i>Irf866</i> , <i>Irf867</i> , <i>Irf868</i> , <i>Irf869</i> , <i>Irf870</i> , <i>Irf871</i> , <i>Irf872</i> , <i>Irf873</i> , <i>Irf874</i> , <i>Irf875</i> , <i>Irf876</i> , <i>Irf877</i> , <i>Irf878</i> , <i>Irf879</i> , <i>Irf880</i> , <i>Irf881</i> , <i>Irf882</i> , <i>Irf883</i> , <i>Irf884</i> , <i>Irf885</i> , <i>Irf886</i> , <i>Irf887</i> , <i>Irf888</i> , <i>Irf889</i> , <i>Irf890</i> , <i>Irf891</i> , <i>Irf892</i> , <i>Irf893</i> , <i>Irf894</i> , <i>Irf895</i> , <i>Irf896</i> , <i>Irf897</i> , <i>Irf898</i> , <i>Irf899</i> , <i>Irf900</i> , <i>Irf901</i> , <i>Irf902</i> , <i>Irf903</i> , <i>Irf904</i> , <i>Irf905</i> , <i>Irf906</i> , <i>Irf907</i> , <i>Irf908</i> , <i>Irf909</i> , <i>Irf910</i> , <i>Irf911</i> , <i>Irf912</i> , <i>Irf913</i> , <i>Irf914</i> , <i>Irf915</i> , <i>Irf916</i> , <i>Irf917</i> , <i>Irf918</i> , <i>Irf919</i> , <i>Irf920</i> , <i>Irf921</i> , <i>Irf922</i> , <i>Irf923</i> , <i>Irf924</i> , <i>Irf925</i> , <i>Irf926</i> , <i>Irf927</i> , <i>Irf928</i> , <i>Irf929</i> , <i>Irf930</i> , <i>Irf931</i> , <i>Irf932</i> , <i>Irf933</i> , <i>Irf934</i> , <i>Irf935</i> , <i>Irf936</i> , <i>Irf937</i> , <i>Irf938</i> , <i>Irf939</i> , <i>Irf940</i> , <i>Irf941</i> , <i>Irf942</i> , <i>Irf943</i> , <i>Irf944</i> , <i>Irf945</i> , <i>Irf946</i> , <i>Irf947</i> , <i>Irf948</i> , <i>Irf949</i> , <i>Irf950</i> , <i>Irf951</i> , <i>Irf952</i> , <i>Irf953</i> , <i>Irf954</i> , <i>Irf955</i> , <i>Irf956</i> , <i>Irf957</i> , <i>Irf958</i> , <i>Irf959</i> , <i>Irf960</i> , <i>Irf961</i> , <i>Irf962</i> , <i>Irf963</i> , <i>Irf964</i> , <i>Irf965</i> , <i>Irf966</i> , <i>Irf967</i> , <i>Irf968</i> , <i>Irf969</i> , <i>Irf970</i> , <i>Irf971</i> , <i>Irf972</i> , <i>Irf973</i> , <i>Irf974</i> , <i>Irf975</i> , <i>Irf976</i> , <i>Irf977</i> , <i>Irf978</i> , <i>Irf979</i> , <i>Irf980</i> , <i>Irf981</i> , <i>Irf982</i> , <i>Irf983</i> , <i>Irf984</i> , <i>Irf985</i> , <i>Irf986</i> , <i>Irf987</i> , <i>Irf988</i> , <i>Irf989</i> , <i>Irf990</i> , <i>Irf991</i> , <i>Irf992</i> , <i>Irf993</i> , <i>Irf994</i> , <i>Irf995</i> , <i>Irf996</i> , <i>Irf997</i> , <i>Irf998</i> , <i>Irf999</i> , <i>Irf1000</i> , <i>Irf1001</i> , <i>Irf1002</i> , <i>Irf1003</i> , <i>Irf1004</i> , <i>Irf1005</i> , <i>Irf1006</i> , <i>Irf1007</i> , <i>Irf1008</i> , <i>Irf1009</i> , <i>Irf1010</i> , <i>Irf1011</i> , <i>Irf1012</i> , <i>Irf1013</i> , <i>Irf1014</i> , <i>Irf1015</i> , <i>Irf1016</i> , <i>Irf1017</i> , <i>Irf1018</i> , <i>Irf1019</i> , <i>Irf1020</i> , <i>Irf1021</i> , <i>Irf1022</i> , <i>Irf1023</i> , <i>Irf1024</i> , <i>Irf1025</i> , <i>Irf1026</i> , <i>Irf1027</i> , <i>Irf1028</i> , <i>Irf1029</i> , <i>Irf1030</i> , <i>Irf1031</i> , <i>Irf1032</i> , <i>Irf1033</i> , <i>Irf1034</i> , <i>Irf1035</i> , <i>Irf1036</i> , <i>Irf1037</i> , <i>Irf1038</i> , <i>Irf1039</i> , <i>Irf1040</i> , <i>Irf1041</i> , <i>Irf1042</i> , <i>Irf1043</i> , <i>Irf1044</i> , <i>Irf1045</i> , <i>Irf1046</i> , <i>Irf1047</i> , <i>Irf1048</i> , <i>Irf1049</i> , <i>Irf1050</i> , <i>Irf1051</i> , <i>Irf1052</i> , <i>Irf1053</i> , <i>Irf1054</i> , <i>Irf1055</i> , <i>Irf1056</i> , <i>Irf1057</i> , <i>Irf1058</i> , <i>Irf1059</i> , <i>Irf1060</i> , <i>Irf1061</i> , <i>Irf1062</i> , <i>Irf1063</i> , <i>Irf1064</i> , <i>Irf1065</i> , <i>Irf1066</i> , <i>Irf1067</i> , <i>Irf1068</i> , <i>Irf1069</i> , <i>Irf1070</i> , <i>Irf1071</i> , <i>Irf1072</i> , <i>Irf1073</i> , <i>Irf1074</i> , <i>Irf1075</i> , <i>Irf1076</i> , <i>Irf1077</i> , <i>Irf1078</i> , <i>Irf1079</i> , <i>Irf1080</i> , <i>Irf1081</i> , <i>Irf1082</i> , <i>Irf1083</i> , <i>Irf1084</i> , <i>Irf1085</i> , <i>Irf1086</i> , <i>Irf1087</i> , <i>Irf1088</i> , <i>Irf1089</i> , <i>Irf1090</i> , <i>Irf1091</i> , <i>Irf1092</i> , <i>Irf1093</i> , <i>Irf1094</i> , <i>Irf1095</i> , <i>Irf1096</i> , <i>Irf1097</i> , <i>Irf1098</i> , <i>Irf1099</i> , <i>Irf1100</i> , <i>Irf1101</i> , <i>Irf1102</i> , <i>Irf1103</i> , <i>Irf1104</i> , <i>Irf1105</i> , <i>Irf1106</i> , <i>Irf1107</i> , <i>Irf1108</i> , <i>Irf1109</i> , <i>Irf1110</i> , <i>Irf1111</i> , <i>Irf1112</i> , <i>Irf1113</i> , <i>Irf1114</i> , <i>Irf1115</i> , <i>Irf1116</i> , <i>Irf1117</i> , <i>Irf1118</i> , <i>Irf1119</i> , <i>Irf1120</i> , <i>Irf1121</i> , <i>Irf1122</i> , <i>Irf1123</i> , <i>Irf1124</i> , <i>Irf1125</i> , <i>Irf1126</i> , <i>Irf1127</i> , <i>Irf1128</i> , <i>Irf1129</i> , <i>Irf1130</i> , <i>Irf1131</i> , <i>Irf1132</i> , <i>Irf1133</i> , <i>Irf1134</i> , <i>Irf1135</i> , <i>Irf1136</i> , <i>Irf1137</i> , <i>Irf1138</i> , <i>Irf1139</i> , <i>Irf1140</i> , <i>Irf1141</i> , <i>Irf1142</i> , <i>Irf1143</i>	

Model-system	Dose	Exposure duration	Methods	Key findings	References
Male Wistar rats	Fructose content provides 60% of calories in diet per day	2 weeks	mRNA expression assessed by northern blot	Decreased expression of <i>Cat</i> and <i>Sod1</i> in the liver and <i>Cat</i> in the heart; reductions in catalase (cat) and cu-ZnSOD1 activity were detected in skeletal muscle and adipose tissues	Cavarape et al., 2001
Male C57BL/6 mice	60% fructose diet per day	6, 10, and 20 weeks	mRNA expression measured using qPCR	No effect on thioredoxin-2 gene expression level; at 6 weeks of exposure, β -myosin gene expression remained unchanged; at 10 weeks, non-significant mRNA expression levels of β -myosin, and NADPH oxidase subunit, Nox2 by 16.8-fold; at 20 weeks, gene expression levels of β -myosin was lowered, and Nox2 was similar for the control and fructose-treated groups	Mellor et al., 2010
Male Wistar rats	60% fructose chow in diet per day	24 weeks	mRNA expression measured using qPCR; myosin 6 protein level determined by proteomics	Myosin 6 protein level was increased after fructose intake; <i>Elovl6</i> and <i>Myh6</i> also increased; Creatine kinase, creatine kinase-MB, and lactate dehydrogenase levels were not significantly different; 45% decrease in cardioliipin	Szucs et al. 2019
Spontaneously hypertensive rats	60% fructose	12 weeks	Protein expression measured by immunoblotting	NADPH oxidase subunit gp91 ^{phox} and angiotensin II type I receptor levels increased in the RVLN neuron and there was a decrease in extracellular SOD expression	Wu et al. 2017

TABLE 3. DHA exposures across various models.

Model-system	Dose	Key findings	References
Cell models			
A375P	5 mM	Inhibited cell growth; increases in ROS; no DNA damage; cell cycle arrest; delayed induction of apoptosis; increased mitochondrial polarization	Smith <i>et al.</i> , 2018
HaCaT	5 to 100 mM	No change in cell proliferation with 25 mM dose after 3 hr; cell cycle arrest (50% increase of cells in the G2/M); doses greater than 25 mM induced cell death; apoptosis; increase in DNA strand breaks	Petersen <i>et al.</i> , 2004
HaCaT	Cell viability analysis by flow cytometry and cell proliferation: ≤ 50 mM; detection of intracellular oxidative stress: ≤ 40 mM; comet assay (alkaline single cell gel electrophoresis): 20 mM; detection of γ -H2AX (S139): ≤ 40 mM	Impaired cell viability, proliferation, and cell cycle progression, increased gene expression of <i>HMOX1</i> due to oxidative stress, increased <i>XRCC2</i> and <i>ERCC3</i> gene expression due to DNA damage, increased AGE formation, increased ROS (only for greater than 40 mM)	Perer <i>et al.</i> , 2020
HEK293T			
HEK293T	5 mM	Cell cycle arrest confirmed by increased cyclin A2 and cyclin B1 levels; no apoptosis as exposure did not lead to cleavage of PARP1 or Caspase 3; autophagy confirmed with increase in LC3BII to LC3BI ratio and SIRT1 expression; reduced mitochondrial membrane potential after 24 hr exposure; initial decline in OCR; decline in ECAR after 24 hr, decreased ATP production and lactate production; NAD ⁺ /NADH cofactor imbalances	Smith <i>et al.</i> , 2019
Animal model systems, human samples, and bacteria			
C57BL/6 mice	8 mM	Exogenous DHA readily enter cells and tissues and form metabolites	Moreno <i>et al.</i> , 2014
Sprague-Dawley rats	80 mM of hyperpolarized [2- ¹³ C] DHA	Generation of different metabolites in liver and kidneys; higher levels of DHA and DHAS in the kidney than the liver	Marco-Rius <i>et al.</i> , 2017
Skin biopsy samples from pig	5, 10, and 20% DHA	DHA increases free radical production by 180% in UV-exposed skin relative to the control untreated group	Jung <i>et al.</i> , 2008
Human serum albumin	Reaction mixtures included 2, 10, or 30 mM of each DHA or DHAP and 35 mg of HAS	HSA is shown to undergo glycation by DHA	Seneviratne <i>et al.</i> 2012
Salmonella typhimurium strain TA100	8% DHA	DHA cytotoxicity with and without metabolic activation; DHA is mutagenic and can lead to DNA damage	Pham <i>et al.</i> , 1979

